Accepted Manuscript

Synthesis and biological evaluation of novel 2-arylvinyl-substituted naphtho[2,3-*d*]imidazolium halide derivatives as potent antitumor agents

Qingyun Wei, Ju Li, Feng Tang, Yin Yin, Yong Zhao, Qizheng Yao

PII: S0223-5234(17)31014-0

DOI: 10.1016/j.ejmech.2017.12.008

Reference: EJMECH 9986

To appear in: *European Journal of Medicinal Chemistry*

Received Date: 14 April 2017

Revised Date: 2 December 2017

Accepted Date: 2 December 2017

Please cite this article as: Q. Wei, J. Li, F. Tang, Y. Yin, Y. Zhao, Q. Yao, Synthesis and biological evaluation of novel 2-arylvinyl-substituted naphtho[2,3-*d*]imidazolium halide derivatives as potent antitumor agents, *European Journal of Medicinal Chemistry* (2018), doi: 10.1016/j.ejmech.2017.12.008.

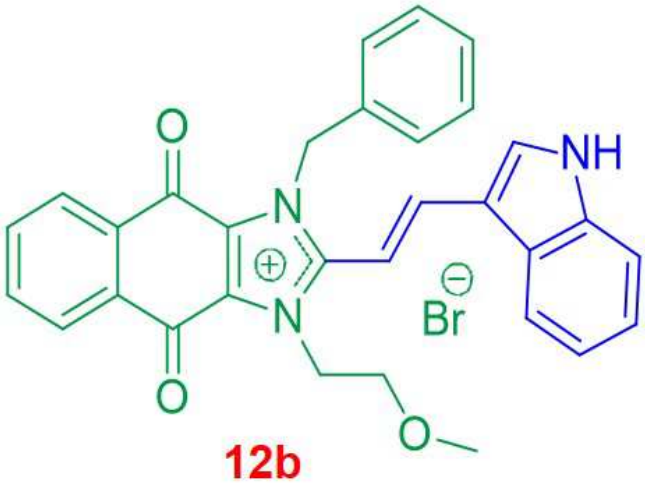

12b

IC_{50} (μM):
0.128 ± 0.017 (PC-3)
0.212 ± 0.029 (A375)
0.059 ± 0.011 (HeLa)

Apoptosis

Anti-tumor

Anti-tubulin

Synthesis and biological evaluation of novel 2-arylvinyl-substituted naphtho[2,3-*d*]imidazolium halide derivatives as potent antitumor agents

Qingyun Wei[a], Ju Li[a], Feng Tang[b], Yin Yin[b], Yong Zhao[b, **], Qizheng Yao[a, *]

[a] Department of Medicinal Chemistry, China Pharmaceutical University, Nanjing 210009, PR China

[b] MtC Biopharma, Co., Ltd, Nanjing 210042, PR China

[*] Corresponding author. Tel./fax: +86 25 86634730

[**] Corresponding author. Tel./fax: +86 13952026874

E-mail address: qz_yao@163.com (Q. Yao), zhaoyong@mtcbiopharma.com (Y. Zhao)

This paper is dedicated to Prof. Wolfgang Pfleiderer for the occasion of his 90th birthday.

Abstract

Two series of novel 2-arylvinyl-naphtho[2,3-*d*]imidazol-3-ium iodide derivatives and 2-arylvinyl-naphtho[2,3-*d*]imidazol-3-ium bromide derivatives were designed and synthesized by the structural combination of YM155 with stilbenoids. All compounds were tested for anti-proliferative activity against PC-3, A375 and HeLa human cancer cell lines. Two of the compounds were selected for further investigation: **12b,** which showed potent cytotoxicity against the three tested cell lines with IC_{50} values in the range of 0.06-0.21 μM, and **7l**, which displayed excellent selectivity for PC-3 cells with an IC_{50} of only 22 nM. Western blot analysis results indicated that both **12b** and **7l** suppress the expression of Bcl-2 and Survivin proteins, which helps induce apoptosis. As determined by the percent of Annexin V-FITC-positive apoptotic cells, **12b** was not only significantly more effective than **7l** at a concentration of 100 nM in PC-3 cells but also induced apoptosis in a dose-dependent manner with more potency than **7l** at a concentration of 1000 nM in A375 cells. Therefore, compound **12b** was chosen for further in-depth studies investigating the mechanism of apoptosis. The results showed that it could activate caspase-3, hydrolyze PARP, and even inactivate ERK. Moreover, **12b** arrested A375 cells at S phase in a time-dependent and dose-dependent manner, while having a visible effect on microtubule dynamics. In addition, (*E*)-2-(2-(1*H*-indol-3-yl)vinyl)-1-benzyl-3-(2-methoxyethyl)-4,9-dioxo-4,9-dihydro-1*H*-naphtho[2,3-d]imidazol-3-ium bromide (**12b**) exhibited significant antitumor activity when evaluated in a subcutaneous solid tumor model. Our study reveals that 2-arylvinyl-substituted

naphtho[2,3-d]imidazolium scaffolding is a promising new entity for the development of multi-target anticancer drugs.

Keywords：naphth[2,3-*d*]imidazol-3-ium; arylvinyl; survivin inhibitor; antitumor drugs

1. Introduction

Survivin, a member of the Inhibitors of Apoptosis Protein (IAP) family, participates in mitosis, apoptosis, and cellular stress response in mammalian cells [1]. Survivin is typically only expressed during embryonic development and is absent in most normal and terminally differentiated tissues. Several studies have shown that survivin is selectively over-expressed in most human tumors and associated with multiple-drug resistance, increased tumor recurrence, and shorter survival times, which make it an attractive target for cancer therapeutics. Targeted therapies that seek to inhibit survivin expression have been utilized in an experimental setting; these studies have used antisense oligonucleotides (LY2181308[2]) or siRNA (EZN-3042[3]), vaccination strategies (EMD640744[4], DPX-0907[5]) and small molecule inhibitors (YM155[6], FL118[7]), which have all yielded promising results to date. All three therapeutic strategies have reached clinical trials, including the use of the small molecule inhibitor YM155 (Sepantronium Bromide) for the treatment of solid tumors and lymphomas [8].

YM155, a novel small molecule inhibitor, belongs to the group of 4,9-dihydro-4,9-dioxo-1*H*-naphtho[2, 3-*d*] imidazolium halide derivative. It blocks the expression of the survivin protein by directly inhibiting of *survivin* promoter [9, 10]. Preclinical studies show that YM155 at nanomolar concentrations suppress survivin expression and inhibit the growth of p53-deficient cancer cells. It was also demonstrated to have antitumor activity in human prostate, pancreatic, and lung cancer xenografts in mice [6]. Researchers have found that the physiological target of YM155 may be the RNA-binding protein interleukin enhancer-binding factor-3 (ILF3/NF110) or a zinc finger transcription factor that preferentially binds GC-rich DNA sequences [11, 12]. YM155 is currently being investigated in a phase Ⅱ clinical trials in combination with chemotherapy[13]. It has been used in combination with carboplatin and paclitaxel to target NSCLC [14]. The combination of YM155 with docetaxel has also shown great efficacy in making melanoma cells sensitive to anticancer drugs [15]. Along with the inhibition of survivin, YM155 has also been shown to exert a synergistic anti-neoplastic effect in combination with taxanes and platinum drugs in earlier studies.

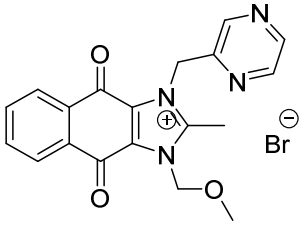

YM155

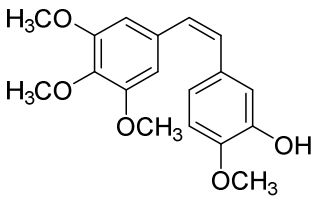

Combretastatin A-4

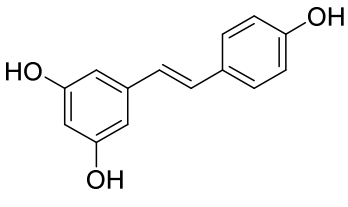

Resveratrol

As the body of data in clinical research grows, novel survivin antagonists are expected to have broad activity in various tumor types, tolerable side-effects, and synergistic efficacy with conventional anticancer treatment [1]. As we gain more understanding of the pathogenesis of human cancers and the interrelated signaling pathways involved in tumor cells, single-target inhibitors have proven to be insufficient in achieving the desired therapeutic effect. In this regard, our interest is focused on developing a new compound by utilizing the structural properties of YM155 in combination with other traditional anticancer drugs.

Stilbene derivatives, including combretastatin and resveratrol, are found in many natural products with diverse applications and biological activities. Combretastatin binds to colchicine sites and act as a tumor vascular-disrupting agent by inhibiting tubulin polymerization to block tumor growth [16, 17]. Several derivatives of combretastatin A-4 (CA-4) have entered clinical trials. It is well-known that tubulin polymerization inhibitors that behave similar to CA-4 require two hydrophobic rings in the Z-configuration within the linking bridge to bind to the active site to elicit a response [18-21]. Resveratrol, a polyphenolic stilbene, has long been an important staple in Chinese and Japanese folk medicine [22]. Numerous studies have shown the great potential of resveratrol as a potent chemotherapeutic agent in diverse human diseases, including a wide variety of cancers [23].

In the present study, two series of novel 2-arylvinyl-substituted naphtho[2,3-*d*]imidazolium halide derivatives have been designed, synthesized and evaluated for antitumor activity by anti-proliferative assay in several human cancer cell lines. The current work in this study provides a basis for further structural modification and transformation of potential naphthoquinone-imidazolium compounds.

2. Results and Discussion

2.1 Chemistry

Two groups of target compounds containing quaternary ammonium salts as the key pharmacophore were prepared: the first set included those with iodized salt (**7a-7q**, Schemes 1), and the second consisted of those with bromide salts (**12a-12g**, Schemes 2).

The first group of compounds was prepared as shown in Scheme 1. Amination of the starting material **1** (2,3-dichloro-1,4-naphthoquinone) with ammonia in refluxing ethanol led to the formation of 2-amino-3-chloro-1,4-naphthoquinone (**2**). Then, *N*-acylation of **2** with acetic anhydride in the presence of concentrated H_2SO_4 gave rise to 2-acetamido-3-chloro-1, 4-naphthoquinone (**3**). The required 1-substituted-2-methylnaphth[2,3-*d*]imidazole-4,9-diones **5a** and **5b** were synthesized in two steps from **3** and the suitable fatty primary amines via the corresponding 2-(acylamino)-3-(alkylamino)-1,4-naphthoquinones **4a** and **4b**, respectively. Reaction of **5** with ethyl iodide gave 2-methyl-3-ethyl-naphtho[2,3-*d*]imidazol-3-ium iodide derivatives (**6a-6b**), according to referenced processes [24, 25]. The resulting compound **6** was allowed to react with 2 eq. of various aromatic aldehydes in dioxane to yield the corresponding 2-arylvinyl-naphtho[2,3-*d*]imidazol-3-ium iodide derivatives **7a-7l** as the final products.

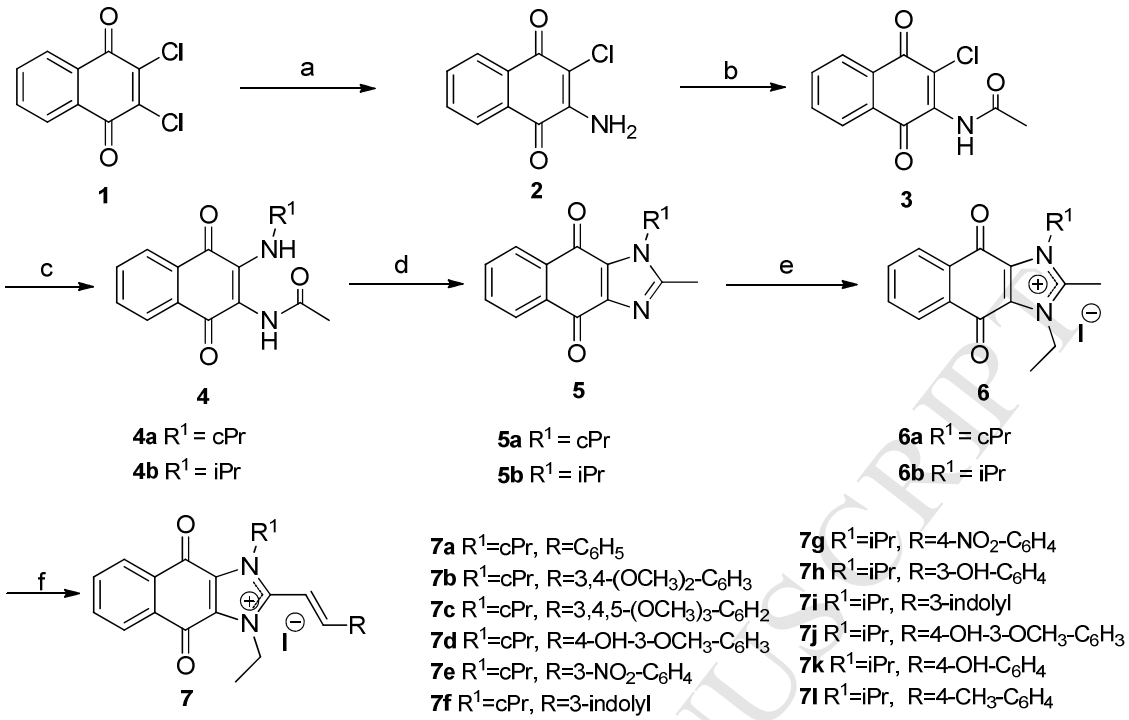

Scheme 1. Synthesis of compounds **7a-l**. Reagents and conditions: a) NH_3, CH_3CH_2OH; b) Ac_2O; c) R_1NH_2, ethanol, 50°C, 30 min; d) NaOH (2N), ethanol, reflux, 30 min; e) ethyl iodide, 2-methoxyethanol, reflux, 4 h; f) R-CHO, pyridine, dioxane, reflux, 2 h.

As shown in Scheme 2, compounds **12a-12g** were prepared following procedures found in cited literature [26]. First, **1** was reacted with 2-methoxyethylamine in a solution of DMF to produce 2-((2-methoxyethyl) amino)-3-chloro-1,4-naphthoquinone (**8**). The resulting product from *N*-acylation of compound **8** by acetic anhydride was subsequently reacted with benzylamine or 3-methoxybenzylamine to produce 2-benzylamino or 2-(3-methyloxybenzyl)amino derivatives (**10a-10b**). Cyclization of **10** in a solution of HBr and 2-methoxyethanol mixture gave rise to 2-methyl-naphtho[2,3-*d*]imidazol-3-ium bromide derivatives (**11a-11b**). Finally, compounds **11** was allowed to reacted with 2 eq. of various aromatic aldehydes in dioxane to yield the final product as 2-arylvinyl-naphtho[2,3-*d*]imidazol-3-ium bromide derivatives **12a-12g**.

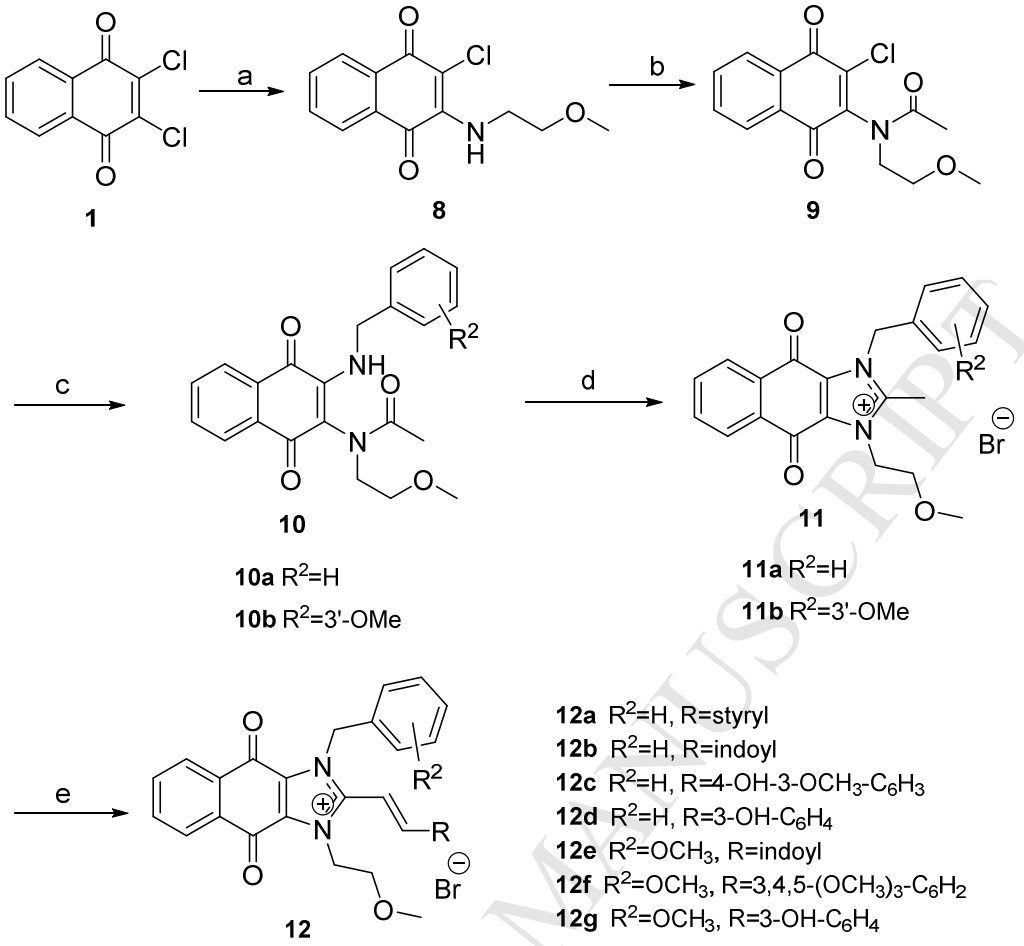

Scheme 2. Synthesis of compounds **12a-g**. Reagents and conditions: a)2-methoxyethylamine, triethylamine, DMF; b) Ac_2O, 50°C, 1 h; c) benzylamine or 3-methoxybenzylamine, ethanol; d) HBr, 2-methoxyethanol, reflux, 2 h; e) R-CHO, pyridine, dioxane, reflux, 2 h.

2.2 Biological activities

2.2.1 In vitro anti-proliferative activity

The in vitro cytotoxicity of synthesized compounds was evaluated by determining the corresponding IC_{50} levels against three human cancer cell lines — PC-3 (prostate), A375 (melanoma) and HeLa (cervix) — compared to the efficacy of YM155 (Table 1).

For the first series of 2-styryl-naphtho[2,3-*d*]imidazol-3-ium iodide derivatives **7a-7l,** compound **7l,** which contains N1-isopropyl and C2-methylstyryl groups, exhibited better cytotoxicity against PC-3 cells than the other compounds. Meanwhile, compound **7i,** which contains N1-isopropyl and C2-3-indolyl groups, showed better cytotoxicity against A375 cells. The presence of N1-cyclopropyl or N1-isopropyl had little influence on the cytotoxic activity against all three cancer lines (**7d** vs **7j**; **7i** vs **7f**).

For the second series of 2-styryl-naphtho[2,3-*d*]imidazol-3-ium bromide derivatives **12a**-**12g,** compound **12b,** which contains N1-benzyl and C2-(indol-3-yl)vinyl groups, exerted the most cytotoxic activity against all three cancer cell lines. Compounds containing a benzyl group expressed better cytotoxicity compared to those with a 3-methoxybenzyl group (**12b** vs **12e**; **12d** vs **12g**).

Overall, compounds containing a C2-(indol-3-yl)vinyl group showed better cytotoxicity compared to those C2-substitued-phenylvinyl group (**7f** among **7a-7f**; **7i** among **7g-7k**; **12b** among **12a-12d**; **12e** among **12e-12g**). Moreover, the cytotoxicity of **12b**, which is added C2-(indol-3-yl)vinyl group on the base of **11a**, was better than **11a** on A375 and HeLa cell lines. The results indicated that the addition of indole ring improves the antiproliferative activity of these derivatives.

Taken together, with IC_{50} values of 0.128 ± 0.017, 0.212 ± 0.029, and 0.059 ± 0.011 μM against PC-3, A375, and HeLa cells, respectively, the results identified **12b** as exhibiting the strongest anticancer activities against all three tested cancer cell lines. Meanwhile, **7l** showed superior cell proliferation inhibition of the PC-3 cell line compared to the other two cancer cell lines tested. The mean IC_{50} value for the PC-3 cell line was 0.022 μM while it was 1.068 μM and 1.12 μM for the A375 and HeLa cell line, respectively (Table **1**). Therefore, we selected two compounds for further studies on their mode of action, **7l** with the highest selectively at PC-3 cell lines, and **12b** with excellent anti-proliferative effects against all three of human cancer cell lines.

Table 1. Inhibitory effect of the new naphtho[2,3-*d*]imidazolium halide compounds on *in vitro* cell growth.

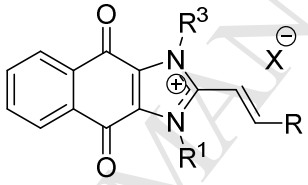

					IC$_{50}$ (μM)[a]		
compd	**X**	**R**	**R^1**	**R^3**	**PC-3**	**A375**	**HeLa**
7a	I	C_6H_5	cPr	CH_3CH_2	0.038 ± 0.001	1.313 ± 0.081	6.54 ± 0.062
7b	I	3,4-$(OCH_3)_2$-C_6H_3	cPr	CH_3CH_2	0.066 ± 0.006	8.000 ± 0.859	13.5 ± 0.200
7c	I	3,4,5-$(OCH_3)_3$-C_6H_2	cPr	CH_3CH_2	0.143 ± 0.011	25.993 ± 3.151	>30
7d	I	4-OH,3-OCH_3-C_6H_3	cPr	CH_3CH_2	0.038 ± 0.000	13.913 ± 1.631	18.5 ± 0.340
7e	I	3-NO_2-C_6H_4	cPr	CH_3CH_2	0.028 ± 0.002	5.357 ± 0.520	11.3 ± 0.340
7f	I	3-indolyl	cPr	CH_3CH_2	0.052 ± 0.003	0.891 ± 0.108	2.05 ± 0.026
7g	I	4-NO_2-C_6H_4	iPr	CH_3CH_2	0.039 ± 0.001	1.429 ± 0.406	9.93 ± 0.265
7h	I	3-OH-C_6H_4	iPr	CH_3CH_2	0.140 ± 0.016	2.940 ± 1.704	13.0 ± 0.000
7i	I	3-indolyl	iPr	CH_3CH_2	0.071 ± 0.002	0.553 ± 0.016	6.12 ± 0.025
7j	I	4-OH,3-OCH_3-C_6H_3	iPr	CH_3CH_2	0.090 ± 0.003	6.579 ± 0.195	>30
7k	I	4-OH-C_6H_4	iPr	CH_3CH_2	0.072 ± 0.007	5.580 ± 0.613	>30
7l	I	4-CH_3-C_6H_4	iPr	CH_3CH_2	0.022 ± 0.001	1.068 ± 0.069	1.12 ± 0.270
12a	Br	C_6H_5(CH=CH)	C_6H_5-CH_2	$CH_3O(CH_2)_2$	0.212 ± 0.004	0.551 ± 0.037	1.28 ± 0.072
12b	Br	3-indolyl	C_6H_5-CH_2	$CH_3O(CH_2)_2$	0.128 ± 0.017	0.212 ± 0.029	0.059 ± 0.011
12c	Br	4-OH,3-OCH_3-C_6H_3	C_6H_5-CH_2	$CH_3O(CH_2)_2$	0.022 ± 0.006	0.536 ± 0.066	1.13 ± 0.145
12d	Br	3-OH-C_6H_4	C_6H_5-CH_2	$CH_3O(CH_2)_2$	0.100 ± 0.004	0.791 ± 0.023	4.86 ± 0.230
12e	Br	3-indolyl	(3-OCH_3-C_6H_4)-CH_2	$CH_3O(CH_2)_2$	0.215 ± 0.010	0.353 ± 0.028	1.37 ± 0.036
12f	Br	3,4,5-$(OCH_3)_3$-C_6H_2	(3-OCH_3-C_6H_4)-CH_2	$CH_3O(CH_2)_2$	0.291 ± 0.030	1.004 ± 0.107	7.50 ± 0.495
12g	Br	3-OH-C_6H_4	(3-OCH_3-C_6H_4)-CH_2	$CH_3O(CH_2)_2$	0.222 ± 0.003	1.118 ± 0.060	7.33 ± 0.096
11a	Br	none	C_6H_5-CH_2	$CH_3O(CH_2)_2$	0.073 ± 0.003	1.141 ± 0.140	10.014 ± 0.263

YM155	Br	none	Pyrazine	$CH_3O(CH_2)_2$	0.005 ± 0.001	0.015 ± 0.003	0.137 ± 0.013

[a]IC_{50} values are the working concentrations (μM) of the tested compounds required to inhibit tumor cell proliferation by 50% after a 48 h treatment; values represent the mean obtained from the dose response curves of three independent experiments.

2.2.2 Compound 12b and 7l suppress the protein expression of Survivin

To investigate whether compound **12b** and **7l** exert their cytotoxicity activity by inhibiting the expression of survivin and other IAP family proteins, A375 cells were treated with these compounds at different concentration for 48 h. As shown in Figure **1**, both compounds **12b** and **7l** suppressed survivin protein expression and stimulated the proteolytic cleavage of procaspase-3. In addition, the anti-apoptotic Bcl-2 protein expression was also decreased.

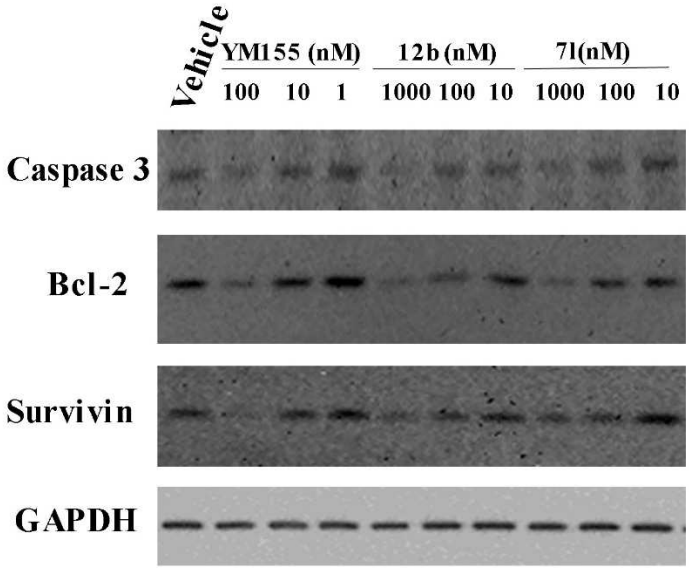

Figure 1. Effect of **12b** and **7l** on apoptosis-related protein expression levels in A375 cells. Cells were incubated with either **12b** or **7l**, harvested at 48 h and whole cell lysates were assayed by immunoblotting. GAPDH was used as a loading control.

2.2.3 Compounds 12b and 7l induce apoptosis.

To determine whether these compounds inhibit tumor cell proliferation through the induction of apoptosis, Annexin V and PI (propidium iodide) dual staining analysis was performed by flow cytometry. After being treated with compound **12b** or **7l** at different concentrations (1, 10, or 100 nM), apoptotic PC-3 cell populations were detected and quantified as the mean ± S.D. of three independent experiments (Figure **2A**).

As depicted in Figure **2B**, A375 cells treated with compound **12b** or **7l** showed an accumulation of Annexin V-positive cells in a concentration-dependent manner compared with vehicle-treated controls. The percent of apoptotic cells in the **12b**-treated group was significantly higher than that of the **7l**-treated group at each concentration level.

These results demonstrate that compound **12b** significantly increased cellular apoptosis in a concentration-dependent manner far better than **7l**, not only PC-3 cell but also A375 cell. Given

that anti-proliferative and apoptosis inducing activity of **12b** better than **7l**, compound **12b** was employed for the further study.

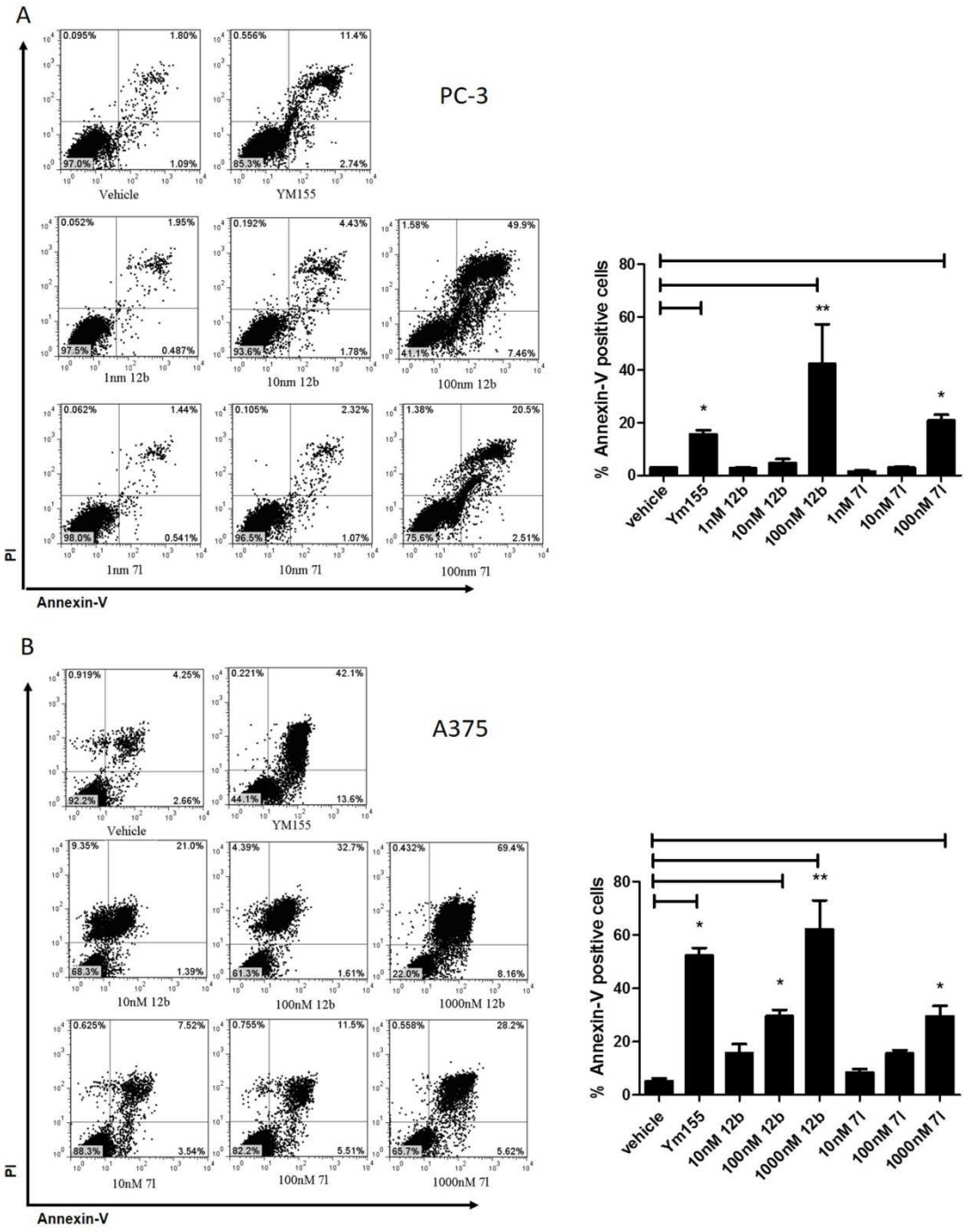

Figure 2. Flow cytometry analysis of apoptosis after treatment PC-3 cell (A) and A375 cell (B) with **12b** and **7l** at the indicated concentrations after 24 h. Vehicle was the negative control group, and cells treated with YM155 (100 nM) was the positive control group. Representative flow cytometric histograms of apoptotic cells (left), and the percent of cells found in the different regions of the biparametric histograms (right) are shown. (Mean ± S.D., n=3; **p*<0.05, ** *p*<0.01).

2.2.4 Effect of Compound 12b on other related proteins expression.

To explore the underlying mechanism of apoptosis that is being induced by compound **12b** in more detail, its effect on other apoptosis-related protein expression levels pertaining to caspase activity was examined. The cleaved form of PARP protein was detected upon exposure to compound **12b**. Similarly, the activity of caspase-3 and caspase-7 was upregulated (Figure **3A** and **3B**), and the expression of p53 was also affected after treatment with compound **12b**. Moreover, the activation of ERK as indicated by the presence of the tyrosine-phosphorylated form p-ERK was also observed after treatment with a high dose of **12b**. Collectively, the data reveals that **12b** induces apoptosis through both the activation of caspase and inactivation of the ERK pathway.

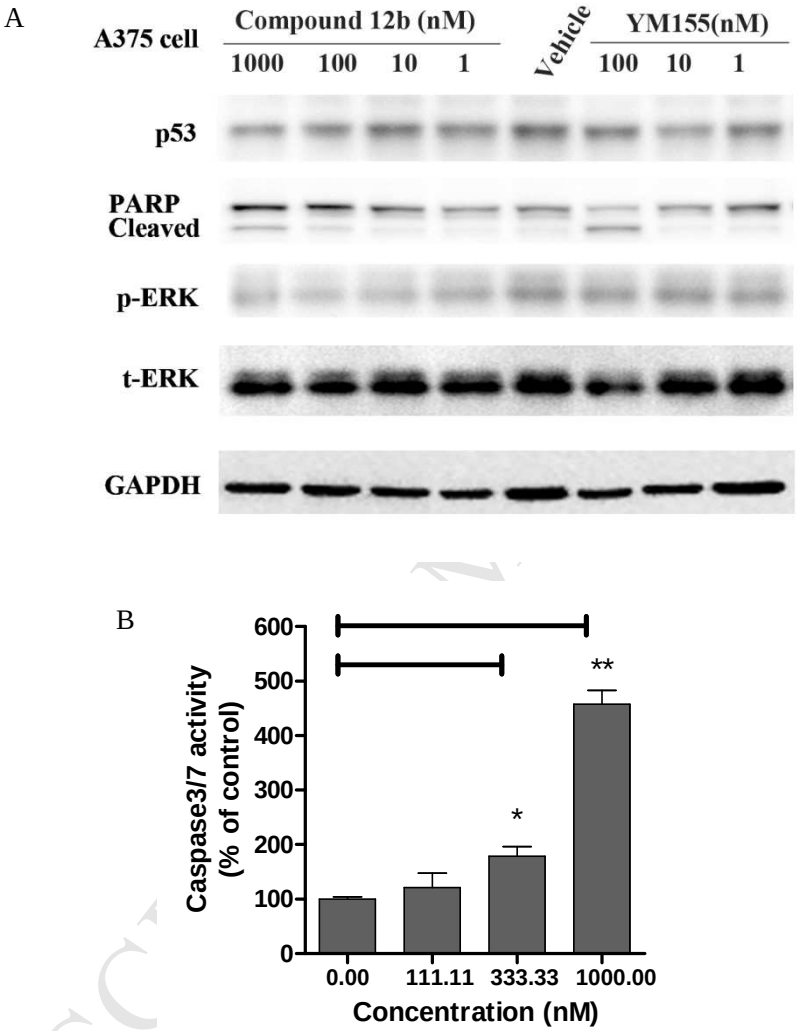

Figure 3. (A) Expression of other apoptosis-related proteins in the induction of apoptosis in A375 cells. A375 cells were incubated with **12b** at four different concentrations, harvested at 48 h and cell lysates were assayed by immunoblotting for the cleavage of PARP, and expression of p-ERK and total ERK. GAPDH were used as a loading control. (B) Caspase enzyme activity was measured after incubation with **12b** for 24 h according to the Caspase-Glo 3/7 assay kit instructions (Mean ± S.D., n=3; *p<0.05, ** p<0.01).

2.2.5 Compounds 12b effects cell cycle distribution.

To further evaluate the effects of compound **12b** on cell growth, cell cycle distribution was determined by flow cytometric analysis of total DNA staining by PI. As shown in Figure **4**, with each increase in either the concentration or the exposure time of compound **12b**, the population of

cells accumulated in S phase gradually increased. After 24 h of treatment with **12b**, the percent of S phase arrested cells increased from 23.62% (vehicle) to 48.06% at 100 nM and 66.08% at the highest concentration (400 nM). In addition, when treated with **12b** at 200 nM, the fraction of cells arrested at S phase was 33.04% and >58.19% after 12 h and 48 h, respectively. The ability of compound **12b** to arrest A375 cells in S/G_2 phase was inferred from these results.

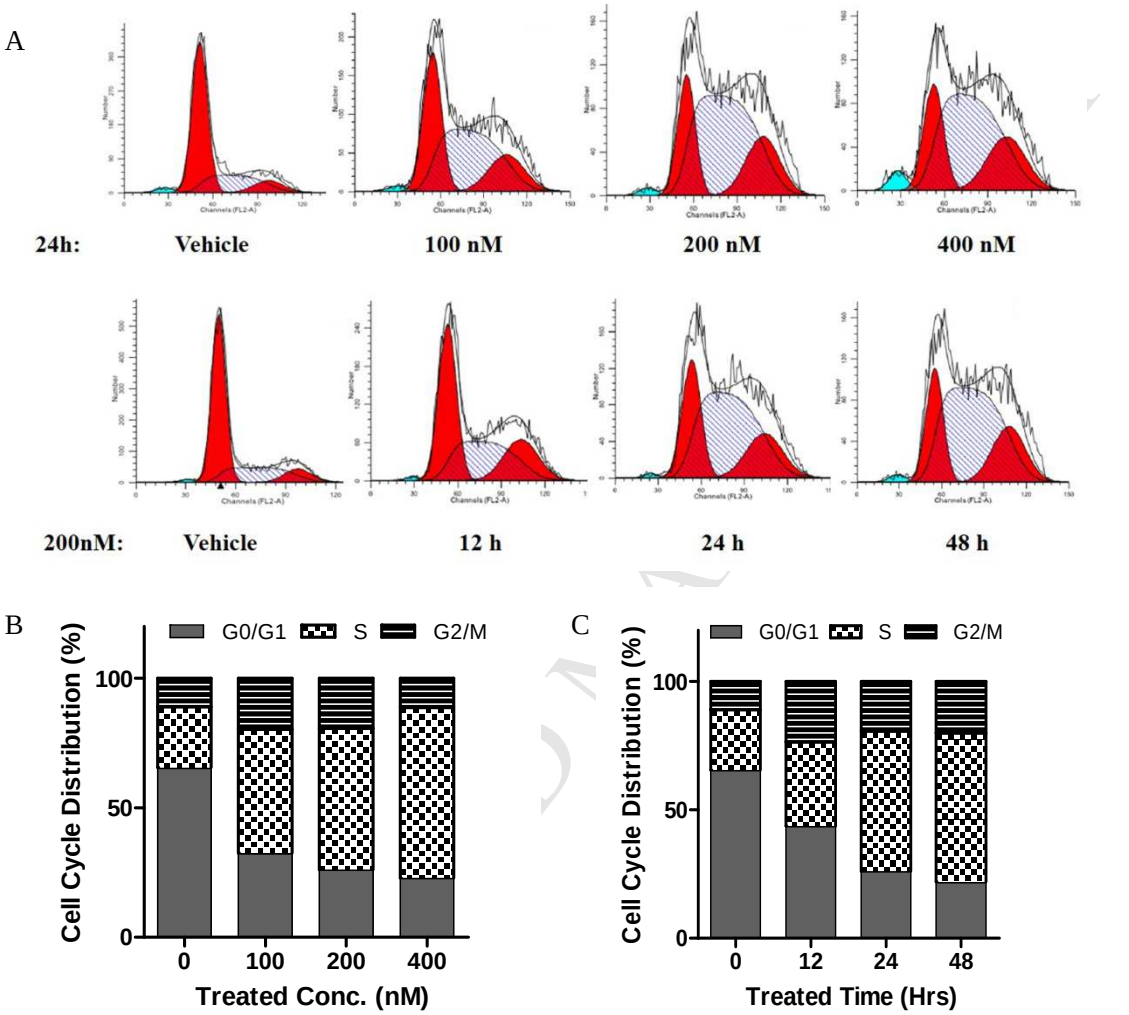

Figure 4. Compound **12b** affects the cell cycle distribution in A375 cells. (A) A375 cells were treatment with **12b** at various concentrations for 24 h and at 200 nM for various time points, respectively. (B, C) After treatment, cells were collected and the DNA content analyzed by flow cytometer.

2.2.6 Effects of compound 12b on the microtubule network.

To get insight into the mechanism of growth inhibition induced by **12b**, we investigated the morphology of microtubules and cytoskeleton by immunofluorescence staining. As shown in Figure **5**, while the control group of A375 cells was spread out with a well-organized microtubule network, the treated group of cells (Paclitaxel group, 300 nM of the **12b** group) was shrunk with improper microtubule bundling; of note, there was no obvious difference observed following incubation with YM155. Furthermore, as highlighted by their rounded morphology, some cells had detached in the presence of either Paclitaxel or the high concentration of **12b** due to the heavy impact of these agents on microtubule depolymerization and cytoskeleton disruption. The result

suggests that tubulin might be a potential target of the antitumor activity of compound **12b** attributable to the arylvinyl-substituent introduced in the structure[27].

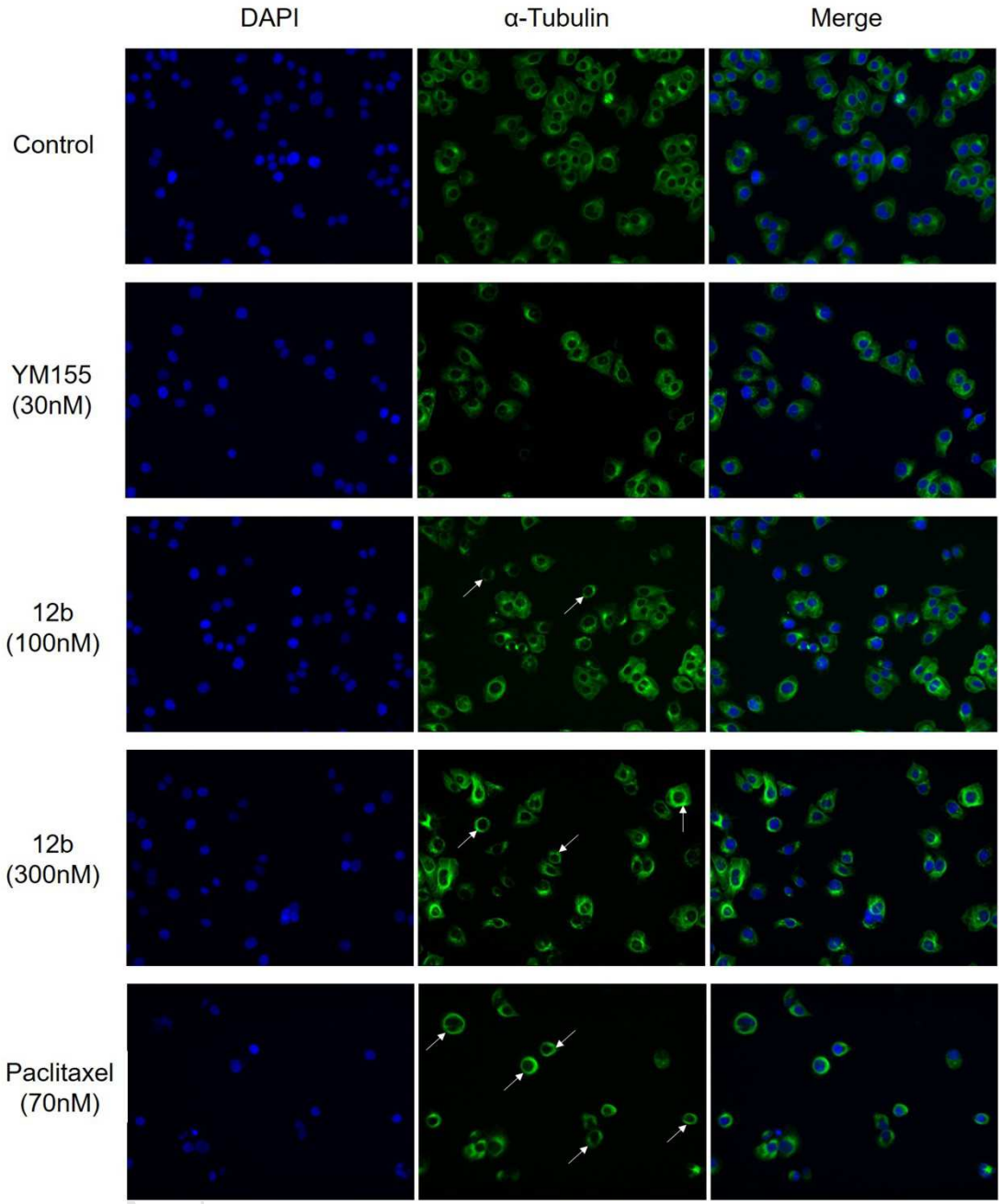

Figure 5. Effect of compound **12b** on the microtubule network of A375 cells. (200×). Cells that were either untreated (control) or treated with compound **12b** at various concentrations for 24 h were stained with α-tubulin and counterstained with 4, 6-diamidino-2-phenylindole (DAPI). Microtubules and unassembled tubulin are shown in green. DNA, stained with DAPI, is shown in blue. Arrows indicate the roundish cells. Paclitaxel, as a common tubulin inhibitor, is a positive control group.

2.2.7 *In vivo* antitumor activity of compound 12b.

To evaluate the *in vivo* antitumor activity of compound **12b**, a subcutaneous solid tumor model were established by injecting Ehrlich's ascites carcinoma (EAC) cells into the thigh of ICR mice [28] [29] Forty-two mice were randomly assigned to six groups 24 h after subcutaneous tumor inoculation. The mice were injected intraperitoneally once a day for 10 consecutive days with the following: the test groups received a dose of either 0.06 mg/kg of **12b**, 0.2 mg/kg of **12b**, 0.6

mg/kg of **12b**, or 0.2 mg/kg of YM155; the positive control group received 30 mg/kg cyclophosphamide (CTX); the vehicle control group received the solvent formula only. The last day the tumors were stripped from mice (Figures **6A**).

As shown in Figures **6B**, the group receiving the high dose (0.6 mg/kg) of compound **12b** had a notable reduction in tumor progression (53.12%) when compared with the group receiving administration of the vehicle only. Moreover, compound **12b** inhibited tumor growth in a dose-dependent manner. Those receiving either YM155 or anticancer drug CTX had a 52.26% and 48.87% tumor reduction, respectively. Hematoxylin and Eosin (HE)-stained tumor (Figures **6C**) showed that the high dose (0.6 mg/kg) of **12b** induce lymphocytes infiltrating into tumors, and surrounding tumor tissue necrosis.

To assess the toxicity of the compound, the weight of important organs was measured and divided by the body weight of each mouse to represent the organ index. Compared with the untreated control group, no remarkable index change was observed in the compound **12b**-treated groups (Figure **6D**). In the CTX group, however, the spleen index and thymus index decreased shapely. Therefore, the data indicated that compound **12b** is effective against solid tumor growth with less side-effect than CTX.

A

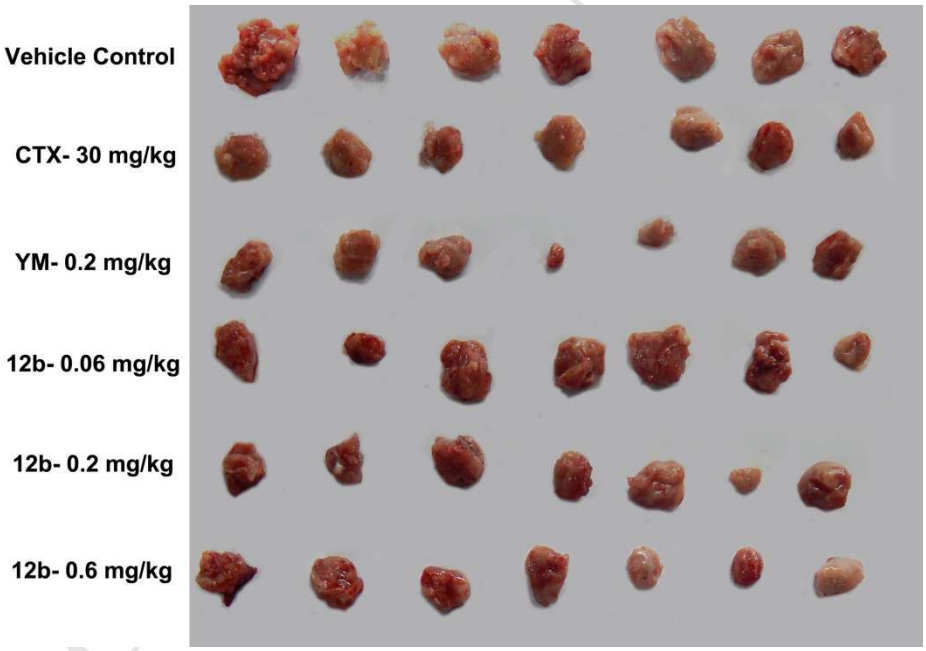

B

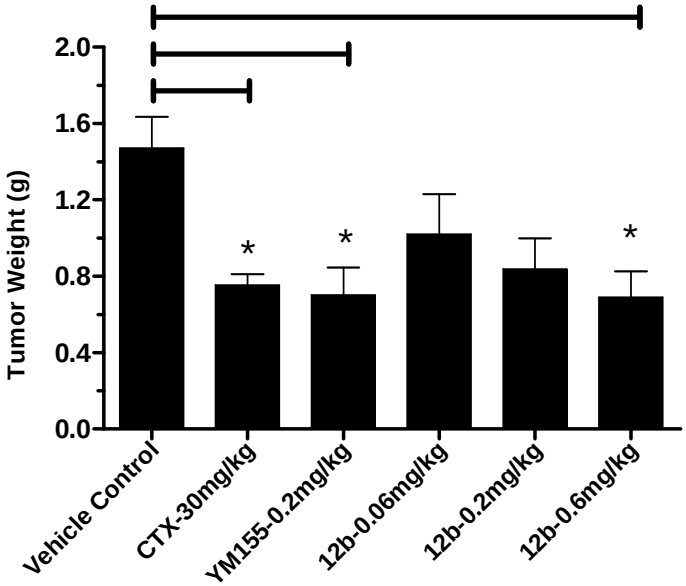
Tumor Weight (g)
2.0
1.6
1.2
0.8
0.4
0.0
*
*
*
Vehicle Control
CTX-30mg/kg
YM155-0.2mg/kg
12b-0.06mg/kg
12b-0.2mg/kg
12b-0.6mg/kg

C

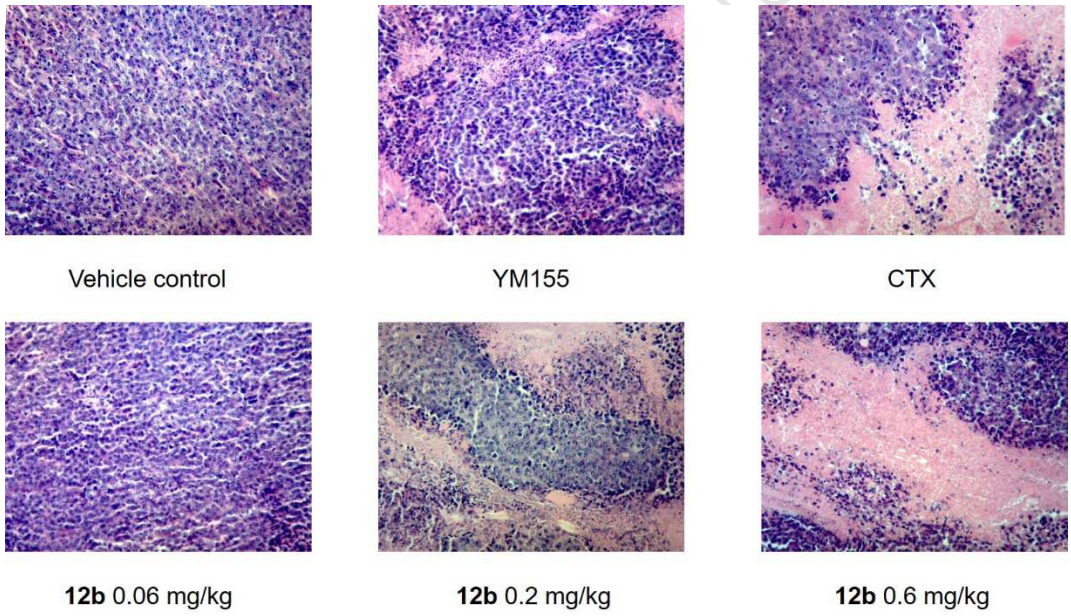
Vehicle control
YM155
CTX
12b 0.06 mg/kg
12b 0.2 mg/kg
12b 0.6 mg/kg

D

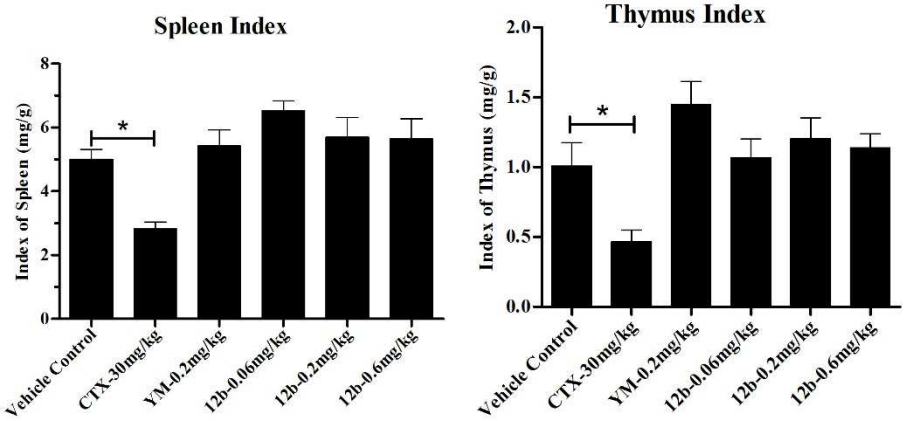
Spleen Index
Index of Spleen (mg/g)
8
6
4
2
0
*
Vehicle Control
CTX-30mg/kg
YM-0.2mg/kg
12b-0.06mg/kg
12b-0.2mg/kg
12b-0.6mg/kg
Thymus Index
Index of Thymus (mg/g)
2.0
1.5
1.0
0.5
0.0
*
Vehicle Control
CTX-30mg/kg
YM-0.2mg/kg
12b-0.06mg/kg
12b-0.2mg/kg
12b-0.6mg/kg

Figure 6. Inhibition of subcutaneous solid tumor growth in vivo by compound **12b** and YM155. (A) Picture of the stripping tumor from mice. (B) The effect of 12b and YM155 on tumor weight was significantly different compared with the vehicle control by the t-test (Mean ± S.D., n=7; *, $P < 0.05$). (C) Histological appearance of the tumor. (D) Effect of 12b against spleen and thymus index (*, $P < 0.05$). CTX, a common clinical agent, was used as a positive control of the study design.

3. Conclusion

Two novel series of 2-arylvinyl-substituted naphtho[2,3-d]imidazolium derivatives have been successfully synthesized and screened for their antitumor activity against three human cancer cell lines. The result revealed that although most of the new compounds show good activity with IC_{50} values below 10 μM, compound **12b** displayed the strongest overall activity with IC_{50} values of 0.128 ± 0.017, 0.212 ± 0.029, and 0.059 ± 0.011 μM against PC-3, A375, and HeLa cell lines, respectively. **7l** showed the strongest activity against PC-3 cells with an IC_{50} value of only 0.022 μM. Additionally, both **7l** and **12b** exhibited potent suppression of Survivin protein expression.

Furthermore, the rate at which apoptosis was induced in PC-3 or A375 cells was higher after treatment for 24 h with **12b** than with **7l**. Compound **12b** was found to induce apoptosis, arrest cell cycle progression at S phase, and lead to the depolymerization of microtubules and disruption of the cytoskeleton in A375 cells. The underlying mechanism for this anticancer activity was associated with a decrease in the expression of anti-apoptosis protein Bcl-2, hydrolysis of PARP, inactivation of ERK, and activation of caspase-3 and caspase-7. *In vivo* tests demonstrated that compound **12b** provides effective antitumor activities with low immunotoxicity. Overall, these results show that compound **12b**, a structural modification from YM155, will lead to the promising development of new anticancer drugs. Studies on the properties of PK (pharmacokinetic) / PD (pharmacodynamic) and Toxicology are already in progress.

4. Experimental protocols

4.1. General

Melting points were determined in open capillaries using the MEL-TEMP II Melting Point apparatus and are uncorrected values. Electrospray ionization (ESI) mass spectrometry data were measured on an HP 1100 IC/MSD and reported as *m*/*z*. Elemental analyses were obtained using the Elementar Vario EL III. NMR spectra were recorded with a BRUKER AV spectrometer at 300 MHz for ^{1}H NMR and 100 MHz for ^{13}C NMR. The chemical shifts are reported in parts per million (ppm), and the coupling constants (*J*) are expressed in hertz (Hz) using trimethylsilane as the internal standard. Splitting patterns are described as singlet (s), doublet (d), triplet (t), quartet (q), quintet, broad (br) or multiplet (m). Reactions were monitored by analytical thin layer chromatography, and the products were visualized by UV light.

2,3-Dichloro-1,4-naphthoquinone was purchased from TCI (Shanghai) Development Co., Ltd. Known compounds **2** and **3** (see Scheme 1) were prepared from appropriate 2,3-dichloro-1,4-naphthoquinone according to previously published procedures [25]. The synthesis of **9** (see Scheme 2) was carried out according to Ref. [30]. All solvents were distilled before they were used, and all other reagents were obtained from commercial suppliers and were of analytical grade. Silica gel (100-200 mesh) used in column chromatography was provided by Tsingtao Marine Chemistry Co. Ltd..

4.2. Synthesis

4.2.1. Experimental procedures for Scheme 1

4.2.1.1 Synthesis of compounds 4a-4b

General procedure: To a solution of 2-acetamido-3-chloro-1,4-naphthoquinone (**3**) (8 mmol) in ethanol (20 mL) was added dropwise the appropriate primary amines (2 equivalents). The reaction solution color turned from yellow to red. The mixture was stirred at 50°C for 30 min, and then cool to room temperature. The resulting precipitated solid was filtered, washed with cooled ethanol. The crude product was purified through recrystallization from ethanol to afford **4a**-**4b**.

*2-(Acylamino)-3-(cyclopropylamino)-1,4-naphthoquinones (**4a**).* According to the general procedure, compound **3** was treated with cyclopropylamine, and purification by recrystallization from ethanol gave compound **4a.**

Yield: 87.1%; orange red powder; mp: 140-141 °C; ^{1}H NMR ($CDCl_3$, 400MHz) δ: 8.01-8.09(m, 2H), 7.59-7.72(m, 2H), 7.20(s, 1H), 6.23(s, 1H), 2.95(s, 1H), 2.23(s, 3H), 0.78(s, 2H), 0.66(s, 2H); ESI-MS: *m/z* 271.0 $[M+H]^+$, $C_{15}H_{14}N_2O_3$ (MW=270.1).

*2-(Acylamino)-3-(isopropylamino)-1,4-naphthoquinones (**4b**).* According to the general procedure, compound **3** was treated with isopropylamine, and purification by recrystallization from ethanol gave compound **4b.**

Yield: 81.6%; red powder; mp: 149-151 °C; ^{1}H NMR (DMSO-d_6, 400MHz) δ: 9.08(s, 1H), 7.96-8.01(m, 2H), 7.73-7.87(m, 2H), 6.43(d, *J*=8.4Hz, 1H), 4.09-4.14(m, 1H), 2.03(s, 3H), 1.19(d, *J*=6.2Hz, 6H); ESI-MS: *m/z* 273.0 $[M+H]^+$, $C_{15}H_{16}N_2O_3$ (MW=272.1).

4.2.1.2 Synthesis of compounds 5a-5b

General procedure: To a solution of compounds **4a**-**4b** (10 mmol) in ethanol (50 mL) was added 2N NaOH (5 mL). The reaction mixture was heated at reflux for 30 min, then diluted with hot water, and added 2N HCl (5 mL). After cooling to room temperature, yellow needle crystals formed and was filtered. The crude product was purified through recrystallization from ethanol to give **5a**-**5b**.

*1-Cyclopropyl-2-methylnaphth[2,3-d]imidazole-4,9-diones (**5a**).*

Yield: 87.3%; yellow solid; mp: 210-212 °C; ^{1}H NMR ($CDCl_3$, 400MHz) δ: 8.13-8.15(m, 2H), 7.69-7.73(m, 2H), 3.34-3.38(m, 1H), 2.65(s, 3H), 1.36-1.42(m, 2H), 1.02-1.06(m, 2H); ESI-MS: *m/z* 253.0 $[M+H]^+$, $C_{15}H_{12}N_2O_2$ (MW=252.1).

*1-Isopropyl-2-methylnaphth[2,3-d]imidazole-4,9-diones (**5b**).*

Yield: 82.7%; yellow solid; mp: 240-241 °C; ^{1}H NMR ($CDCl_3$, 400MHz) δ: 8.22-8.15(m, 2H), 7.69-7.74(m, 2H), 5.18(br, 1H), 2.65(s, 3H), 1.66(s, 3H), 1.64(s, 3H); ESI-MS: *m/z* 255.0 $[M+H]^+$, $C_{15}H_{14}N_2O_2$ (MW=254.1).

4.2.1.3 Synthesis of compounds 6a-6b

General procedure: To a solution of compounds **5a**-**5b** (10 mmol) in 2-methoxyethanol (20mL) was added ethyl iodide (1.5 equivalents). The reaction mixture was heated at reflux for 4 h. After cooling, the red precipitate was filtered, washed with ethanol. The crude product was purified through recrystallization from methanol to give **6a-6b** as orange powder.

*1-Cyclopropyl-2-methyl-3-ethyl-4,9-dioxo-4,9-dihydro-1H-naphth[2,3-d]imidazol-3-ium iodide (**6a**).*

Yield: 88.2%; orange powder; mp: 242-243 °C; ^{1}H NMR (DMSO-d_6, 400MHz) δ: 8.195-8.203 (m, 2H), 7.995-8.014(m, 2H), 4.62(m, 2H) 3.66-3.68(m, 1H), 2.92(s, 3H), 1.43(t, *J*=7.0Hz, 3H), 1.41(d, 2H), 1.21(s, 2H); ESI-MS: *m/z* 281.1 $[M-I]^+$,$C_{17}H_{17}IN_2O_2$ (MW=408.2) , $C_{17}H_{17}N_2O_2^+$ (MW=281.1).

*1-Isopropyl-2-methyl-3-ethyl-4,9-dioxo-4,9-dihydro-1H-naphth[2,3-d]imidazol-3-ium iodide (**6b**).*

Yield: 85.9%; orange powder; mp: 233-234 °C; ^{1}H NMR (DMSO-d_6, 400MHz) δ: 8.19-8.23(m, 2H), 8.00-8.03(m, 2H), 5.44(br, 1H), 4.69-4.70(m, 2H), 3.00(s, 3H), 1.66(d, *J*=6.8Hz, 6H), 1.44(t, *J*=7.0Hz, 3H); ESI-MS: *m/z* 283.1 $[M-I]^+$,$C_{17}H_{19}IN_2O_2$ (MW=410.2) , $C_{17}H_{19}N_2O_2^+$ (MW=283.1).

4.2.1.4 Synthesis of compounds 7a-7l

General procedure: A mixture of compounds **6a** (1 mmol), aromatic aldehydes (2 equivalents), 8 mL of dioxane, and 0.4 mL of pyridine was refluxed for 2 h. After cooling to room temperature, the precipitate was filtered off, washed with ethanol, and dried. The crude product was purified through recrystallization from methanol to give **7a-7f** as orange powder.

Compounds **7g-7l** were synthesized from **6b** using the same method.

*(E)-1-Cyclopropyl-2-styryl-3-ethyl-4,9-dioxo-4,9-dihydro-1H-naphth[2,3-d]imidazol-3-ium iodide (**7a**).*

Yield: 91.7%; orange powder; mp: 216-217 °C; ^{1}H NMR(DMSO-*d6*, 300 MHz) δ: 8.22(s, 2H), 8.13-8.30(m, 5H), 7.57(d, *J*=15Hz, 2H), 7.50-7.65(m, 2H), 4.80(s, 1H), 4.10-4.27(m, 2H), 1.37-1.43(m, 4H), 1.12(s, 3H); ESI-MS: *m/z* 369.1 $[M-I]^+$, $C_{24}H_{21}N_2O_2^+$ (MW=369.1); Anal.calcd for $C_{24}H_{21}IN_2O_2 \cdot 0.15HI$ (515.25): C56.00, H4.15, N5.27; Found: C55.92, H4.14, N5.43.

*(E)-1-Cyclopropyl-2-(3,4-dimethoxystyryl)-3-ethyl-4,9-dioxo-4,9-dihydro-1H-naphth[2,3-d]imidazol-3-ium iodide (**7b**).*

Yield: 65.9%; orange red powder; mp: 250 °C; ^{1}H NMR(DMSO-d_6, 300 MHz) δ: 8.19-8.22(m, 2H), 7.98-8.02 (m, 2H), 7.94(d, *J*=15Hz, 1H), 7.49-7.59(m, 2H), 7.35(d, *J*=15Hz, 1H), 7.14(d, *J*=6Hz, 1H), 4.80-4.84(m, 2H), 3.87(s, 1H), 1.38-1.48(m, 4H), 1.08(s, 3H); ESI-MS: *m/z* 429.2 $[M-I]^+$, $C_{26}H_{25}IN_2O_4^+$(MW=429.2); Anal.calcd for $C_{26}H_{25}IN_2O_4 \cdot 0.06HI$ (563.75): C55.35, H4.23, N4.83; Found: C55.36, H4.48, N4.97.

*(E)-1-Cyclopropyl-2-(3,4,5-trimethoxystyryl)-3-ethyl-4,9-dioxo-4,9-dihydro-1H-naphth[2,3-d]imidazol-3-ium iodide (**7c**).*

Yield: 55.9%; red brown powder; mp: 235-236°C; ^{1}H NMR(DMSO-d_6, 300 MHz) δ: 8.02-8.22(m, 2H), 8.00-8.03(m, 2H), 7.92(d, *J*=18Hz, 1H), 7.44(d, *J*=18Hz, 1H), 7.30(s, 2H), 4.80-4.83(m, 2H), 4.27(s, 1H), 3.89(s, 6H), 3.76(s, 3H), 1.39-1.46(m, 4H), 1.09(s, 3H); ^{13}C-NMR (DMSO-d_6, 100MHz) δ: 175.29, 174.96, 173.44, 173.38, 153.28, 150.75, 150.06, 149.33, 140.76, 135.34, 135.01, 133.11, 132.05, 131.40, 130.28, 129.64, 126.92, 106.79, 105.74, 105.20, 60.25, 56.38, 56.34, 42.84, 34.74, 31.36, 11.38; ESI-MS: *m/z* 459.2 $[M-I]^+$, $C_{27}H_{27}IN_2O_5^+$(MW=459.2); Anal.calcd for $C_{27}H_{27}IN_2O_5 \cdot 0.11HI$ (600.18): C53.93, H4.39, N4.40; Found: C54.00, H4.55, N4.67.

*(E)-1-Cyclopropyl-2-(4-hydroxy-3-methoxystyryl)-3-ethyl-4,9-dioxo-4,9-dihydro-1H-naphth[2,3-d]imidazol-3-ium iodide (**7d**).*

Yield: 75.3%; orange powder; mp: 260°C; ^{1}H NMR(DMSO-d_6, 300 MHz) δ: 10.00(s, 1H), 8.20-8.22(m, 2H), 8.01-8.03(m, 2H), 7.93(d, *J*=18Hz, 1H), 7.56(s, 1H), 7.39-7.45(m, 1H), 7.28(d, *J*=18Hz, 1H), 6.93(d, *J*=6Hz, 1H), 4.79-4.81(m, 2H), 4.04-4.06(m, 1H), 3.90(s, 3H), 1.38-1.48(m, 4H), 1.08(s, 3H); ESI-MS: *m/z* 415.2 $[M-I]^+$, $C_{25}H_{23}N_2O_4^+$(MW=415.2); Anal.calcd for $C_{25}H_{23}IN_2O_4 \cdot 0.09HI$ (553.62): C54.15, H3.93, N4.87; Found: C54.21, H4.20, N5.06.

*(E)-1-Cyclopropyl-2-(3-nitrostyry)-3-ethyl-4,9-dioxo-4,9-dihydro-1H-naphth[2,3-d]imidazol-3-ium iodide (**7e**).*

Yield: 90.6%; orange powder; mp: 236-238°C; ^{1}H NMR(DMSO-d_6, 300 MHz) δ: 8.20-8.24(m, 2H), 8.06(d, *J*=15Hz, 1H), 8.01-8.03(m, 3H), 7.56(d, *J*=15Hz, 1H), 7.57-7.58(m, 3H), 4.78-4.81(m, 2H), 4.11-4.15(m, 1H), 1.36-1.45(m, 4H), 0.90-0.95(m, 3H); ^{13}C-NMR (DMSO-d_6, 100 MHz) δ: 174.91, 148.48, 146.38, 146.03, 135.81, 135.77, 135.40, 135.06, 134.51, 131.99, 130.66, 126.99, 126.80, 125.58, 123.35, 110.06, 109.56, 66.33, 43.11, 34.87, 31.37, 14.69, 11.28, 11.07; ESI-MS: *m/z* 414.1 $[M-I]^+$, $C_{24}H_{20}N_3O_4^+$(MW=414.1); Anal.calcd for $C_{24}H_{20}IN_3O_4 \cdot 0.12HI$ (556.39): C51.78, H3.45, N7.24; Found: C51.78, H3.64, N7.55.

*(E)-1-Cyclopropyl-2-(2-(1H-indol-3-yl)vinyl)-3-ethyl-4,9-dioxo-4,9-dihydro-1H-naphth[2,3-d]imidazol-3-ium iodide (**7f**).*

Yield: 94.3%; red powder; mp: 329°C; ^{1}H NMR(DMSO-d_6, 300 MHz) δ: 12.01(s, 1H), 8.29(d, *J*=18Hz, 1H), 8.208.22(m, 2H), 8.14-8.15(m,2H), 8.00-8.00(m, 2H), 7.55-7.58(m, 1H), 7.29-7.31(m, 2H), 7.10(d, *J*=18Hz, 1H), 4.79-4.81(m, 2H), 4.08-4.13(m, 1H), 1.39-1.52(m, 4H), 1.10(s, H3H); ^{13}C-NMR (DMSO-d_6, 100 MHz) δ: 175.08, 173.47, 150.96, 143.51, 137.47, 135.17, 134.83, 133.68, 132.72, 131.93, 131.49, 129.54, 126.78, 126.61, 124.95, 123.24, 121.69, 120.01, 112.95, 112.78, 97.90, 66.33, 42.45, 31.14, 14.29, 11.54; ESI-MS: *m/z* 408.2 $[M-I]^+$, $C_{26}H_{22}IN_3O_2^+$(MW=408.2); Anal.calcd for $C_{26}H_{22}IN_3O_2\cdot 0.05HI$(541.47): C57.60, H3.72, N7.62; Found: C57.64, H4.10, N7.76.

*(E)-1-Isopropyl-2-(4-nitrostyry)-3-ethyl-4,9-dioxo-4,9-dihydro-1H-naphth[2,3-d]imidazol-3-ium iodide (**7g**).*

Yield: 83.1%; yellow powder; mp: 208°C; ^{1}HNMR(DMSO-d_6, 300 MHz) δ: 8.38-8.42(m, 2H), 8.17-8.28(m, 4H), 7.99-8.06(m, 2H), 7.63-7.75(m, 2H), 5.33-5.38(m, 1H), 4.68-4.71(m, 2H), 1.64-1.70(m, 6H), 1.41-1.45(m, 3H); ^{13}C-NMR (DMSO-d_6, 100 MHz) δ: 174.90, 174.08, 148.49, 148.19, 144.56, 139.79, 135.50, 135.09, 131.88, 131.48, 131.09, 129.88, 127.37, 126.78, 124.03, 111.81, 66.33, 54.42, 52.75, 43.94, 42.73, 20.08, 19.61, 14.63; ESI-MS: *m/z* 416.1 $[M-I]^+$, $C_{24}H_{20}N_3O_4^+$(MW=416.1); Anal.calcd for $C_{24}H_{22}IN_3O_4\cdot 0.08HI$ (553.09): C51.96, H4.06, N7.11; Found: C51.95, H4.01, N7.57.

*(E)-1-Isopropyl-2-(3-hydroxystyryl)-3-ethyl-4,9-dioxo-4,9-dihydro-1H-naphth[2,3-d]imidazol-3-ium iodide (**7h**).*

Yield: 75.8%; orange powder; mp: 234-235°C; ^{1}H NMR(DMSO-d_6, 300 MHz) δ: 9.79(s, 1H), 8.03-8.20(m, 4H), 7.35-7.51(m, 4H), 7.30(d, *J*=15Hz, 2H), 6.95(d, *J*=6Hz, 1H), 5.30-5.32(m, 1H), 4.66-4.68(m, 2H), 1.68(d, *J*=6Hz, 6H), 1.46-1.51(m, 3H); ESI-MS: *m/z* 387.2 $[M-I]^+$, $C_{24}H_{23}N_2O_3^+$(MW=387.2); Anal.calcd for $C_{24}H_{23}IN_2O_3\cdot 0.05HI$ (520.47): C55.96, H4.21, N5.00; Found: C55.58, H4.48, N5.40.

*(E)-1-Isopropyl-2-(2-(1H-indol-3-yl)vinyl)-3-ethyl-4,9-dioxo-4,9-dihydro-1H-naphth[2,3-d]imidazol-3-ium iodide (**7i**).*

Yield: 91.6%; red brown powder; mp: 230°C; ^{1}HNMR(DMSO-d_6, 300 MHz) δ: 12.10(s,1H), 8.11-8.27(m, 4H), 8.01-8.08(m, 2H)，7.83(d, *J*=16.5Hz, 1H), 7.54-7.57(m, 1H), 7.25-7.32(m, 2H), 7.05(d, *J*=16.5Hz, 1H), 5.34-5.38(m, 1H), 4.70-4.72(m, 2H), 1.72(d, *J*=6Hz, 6H), 1.51-1.55(m, 3H); ^{13}C-NMR (DMSO-d_6, 100 MHz) δ: 175.03, 174.21, 141.19, 137.36, 135.34, 135.09, 133.01, 127.22, 126.44, 124.73, 123.04, 121.40, 119.92, 112.66, 112.03, 98.74, 66.33, 53.97, 43.63, 39.74,

39.53, 39.32, 20.10, 14.52; ESI-MS: *m/z* 410.2 $[M-I]^+$,$C_{26}H_{24}N_3O_2^+$(MW=410.2); Anal.calcd for $C_{26}H_{24}IN_3O_2 \cdot 0.02HI$ (539.65): C57.83, H4.19, N7.53; Found: C57.80, H4.48, N7.78.

*(E)-1-Isopropyl-2-(4-hydroxy-3-methoxystyryl)-3-ethyl-4,9-dioxo-4,9-dihydro-1H-naphth[2,3-d]imidazol-3-ium iodide (**7j**).*

Yield: 67.8%; orange powder; mp: 225-226°C; ^{1}H NMR(DMSO-d_6, 300 MHz) δ: 9.90(s, 1H), 8.20-8.24(m,2H), 8.01-8.03(m,2H), 7.53(s, 1H), 7.36(t, *J*=18Hz, 2H)，7.22-7.36(m, 1H), 6.91(d, *J*=9Hz, 1H), 5.28-5.32(m, 1H), 4.66-4.68(m, 2H), 3.89(s, 3H), 1.63-1.70(m, 6H), 1.43-1.51 (m, 3H); ^{13}C-NMR (DMSO-d_6, 100 MHz) δ: 174.97, 174.13, 150.31, 149.56, 148.09, 147.35, 135.42, 135.18, 131.85, 131.79, 131.34, 131.14, 127.29, 126.70, 125.28, 123.86, 115.64, 111.86, 103.09, 56.04, 54.10, 43.72, 39.74, 20.06, 14.59; ESI-MS: *m/z* 417.2 $[M-I]^+$,$C_{25}H_{25}N_2O_4^+$(MW=417.2); Anal.calcd for $C_{25}H_{25}IN_2O_4 \cdot 0$,.02HI (546.64): C54.80, H4.18, N4.82; Found: C54.87, H4.61, N5.12.

*(E)-1-Isopropyl-2-(4-hydroxystyryl)-3-ethyl-4,9-dioxo-4,9-dihydro-1H-naphth[2,3-d]imidazol-3-ium iodide (**7k**).*

Yield: 75.8%; yellow powder; mp: 235°C; ^{1}HNMR(DMSO-d_6, 300 MHz) δ: 10.24(s, 1H), 8.02-8.20(m, 4H), 7.78(d, *J*=9Hz, 2H), 7.40(d, *J*=15Hz, 2H), 6.91(d, *J*=9Hz, 2H), 5.30(s, 1H), 4.66-4.68(m, 2H), 1.67(d, *J*=9Hz, 6H), 1.47-1.51(m, 3H); ESI-MS: *m/z* 387.2 $[M-I]^+$,$C_{24}H_{23}N_2O_3^+$(MW=387.2); Anal.calcd for $C_{24}H_{23}IN_2O_3 \cdot C_4H_8O_2$ (601.93): C55.73, H4.73, N4.20; Found: C55.82, H5.19, N4.65.

*(E)-1-Isopropyl-2-(4-methylstyryl)-3-ethyl-4,9-dioxo-4,9-dihydro-1H-naphth[2,3-d]imidazol-3-ium iodide (**7l**).*

Yield: 68.1%; orange powder; mp: 210-212°C; ^{1}H NMR(DMSO-d_6, 300 MHz) δ: 8.21-8.26(m, 2H), 8.02-8.05(m, 2H), 7.92-7.93(m, 2H), 7.52-7.59(m,2H), 7.49(t, *J*=15Hz, 2H), 5.33-5.35(m,1H), 4.67-4.70(m, 2H), 1.68(d, *J*=6Hz, 6H), 1.48-1.52(m, 3H); ESI-MS: *m/z* 385.2 $[M-I]^+$,$C_{25}H_{25}N_2O_2^+$(MW=385.2); Anal.calcd for $C_{25}H_{25}IN_2O_2 \cdot 0.5H_2O$ (521.09): C53.35, H5.05, N5.57; Found: C53.60, H4.72, N5.49.

4.2.2. Experimental procedures for Scheme 2

4.2.2.1 2-Chloro-3-((2-methoxyethyl)amino)-1,4-naphoquinone (8).

To an ice-cold stirred solution of compounds **1** (10 mmol) and triethylamine (1 mL) in DMF (20 mL) was added dropwise 2-methoxyethylamine (12.5 mmol). After the mixture color turned from light yellow to red, the reaction continued at room temperature for 1h, then poured into 300 mL water to form a orange red precipitate. The resulting precipitated solid was filtered, washed with cooled water, and dried.

Yield: 96.1%; orange powder; mp: 82-83°C; ^{1}H NMR (DMSO-d_6, 400MHz) δ: 7.98(m, 2H), 7.75-7.87(m, 2H), 7.25(s, 1H), 3.92-3.94(m, 2H), 3.57(t, J = 5.7Hz, 2H), 3.29-3.38(s, 3H); ESI-MS: *m/z* 266.1 $[M+H]^+$, $C_{13}H_{12}ClNO_3$ (MW=265.1).

4.2.2.2 2-Chloro-3-((2-methoxyethyl)acetylamino)-1,4-naphoquinone (9).

This compound was prepared using a modification of the procedure described by Mastsuhisa [30]. A few drops of concentrated sulfuric acid was added to a solution of compound **8** (10 mmol) in acetic anhydride (3 mL), and the mixture was stirred at 50°C for 1 h. By adding ethanol (3 mL) to the reaction solution, excess acetic anhydride was esterified. After cooling, ethyl acetate was added to the reaction solution and the mixture was washed with water and brine before being dried over anhydrous sodium sulfate. The solvent was evaporated and the residue was crystallized from diethyl ether to give **9**.

4.2.2.3 Synthesis of compounds 10a-10b

To a solution of compound **9** (10 mmol) in ethanol (20 mL) was added 22.5 mmol benzylamine , then the mixture color turned from yellow to red. The reaction solution continued for 1h at room temperature, and then concentrated to dryness under reduced pressure. The crude material was purified on a silica gel column with the gradient eluent to yield compounds **10a**. The elution was petroleum ether/ethyl acetate (v/v from 10:1 to 2:1, based on the polarity of final products).

2-benzylamino-3-((2-methoxyethyl)acetylamino)-1,4-naphoquinone (10a).

^{1}HNMR (DMSO-d_6, 400MHz) δ: 8.12-8.14 (m, H), 8.07-8.09 (m, H), 7.75-7.78 (m, H), 7.65-7.68 (m, H), 7.32-7.39 (m, 4H), 7.27-7.30 (m, H), 6.58 (br, H), 4.80-4.82 (m, H), 4.57-4.60 (m, H), 3.69-3.74 (m, H), 3.42-3.47(m, H), 3.14-3.25 (m, 3H), 1.80-2.04 (m, 3H), 1.5-1.8 (m, 2H); ESI-MS: *m/z* 378.2 $[M]^+$.

To a solution of compound **9** (10 mmol) in ethanol (20 mL) was added 22.5 mmol 3-methoxybenzylamine, then the mixture color turned from yellow to red. The reaction solution continued for 1h at room temperature, and then concentrated to dryness under reduced pressure. The intermediate **10b** was obtained.

4.2.2.4 Synthesis of compounds 11a-11b

Hydrogen bromide (1 mL) was added to a solution of compound **10a** (10 mmol) in 2-methoxyethanol (20 mL), and the mixture was refluxed for 2 h. The reaction solution was cooled and the precipitate was filtered, wash and dried. The crude product was purified through recrystallization from methanol to give **11a** as yellow powder.

*1-benzyl-3-(2-methoxyethyl)-2-methyl-4,9-dioxo-4,9-dihydro-1H-naphth[2,3-d]imidazol-3-ium bromide(**11a**).*

Yield: 80.6%; orange yellow powder; mp: 199-201°C; ^{1}HNMR (DMSO-d_6, 400MHz) δ: 8.16-8.17 (m, 2H), 7.98-8.03 (m, 2H), 7.38-7.43 (m, 3H), 7.31-7.36 (m, 2H), 6.03 (s, 2H), 4.86 (t, *J*=5Hz, 2H), 3.80 (t, *J*=5Hz, 2H), 3.24(s, 3H), 2.84(s, 3H); ESI-MS: *m/z* 361.1 $[M-Br]^+$.

Hydrogen bromide (1 mL) was added to a solution of intermediate **10b** in 2-methoxyethanol (20 mL), and the mixture was refluxed for 2 h. The reaction solution was cooled and condensed to afford crude **11b** as brown liquid, which used immediately for the next step.

4.2.2.5 Synthesis of compounds 12a-12g

General procedure: A mixture of compound **11a** (1 mmol), aromatic aldehydes (2 equivalents), 8 mL of dioxane, and 0.4 mL of pyridine was refluxed for 2 h. After allowing to cool to room temperature, the precipitate was filtered off, washed with ethanol, and dried. The crude product was purified through recrystallized from methanol to give **12a**-**12d** as yellow powder.

Compounds **12e**-**12g** were synthesized from **11b** using the same method.

*1-Benzyl-3-(2-methoxyethyl)-2-((1E,3E)-4-phenylbuta-1,3-dien-1-yl)-4,9-dioxo-4,9-dihydro-1H-naphth[2,3-d]imidazol-3-ium bromide (**12a**).*

Yield: 63.7%; yellow powder; mp: 202°C; ^{1}H NMR(DMSO-d_6, 300 MHz) δ: 8.02-8.22(m, 4H), 7.54-7.62(m, 3H), 7.38-7.42(m, 2H), 7.28-7.35(m, 5H), 7.06(d, *J*=15Hz, 2H), 6.08(s, 2H), 4.81-4.89(m, 2H), 3.93(d, *J*=21Hz, 2H), 3.28-3.30(m, 2H), 3.02(s, 3H); ESI-MS: *m/z* 475.2 $[M-Br]^+$,$C_{31}H_{27}N_2O_3^+$(MW=475.2); Anal.calcd for $C_{31}H_{27}BrN_2O_3\cdot 0.25HBr$ (574.20): C64.09，H4.86，N5.14; Found: C64.23, H4.74, N4.83.

*(E)-1-Benzyl-3-(2-methoxyethyl)-2-(2-(1H-indol-3-yl)vinyl)-4,9-dioxo-4,9-dihydro-1H-naphth[2,3-d]imidazol-3-ium bromide (**12b**).*

Yield: 85.6%; orange powder; mp: 200-202°C; ^{1}H NMR(DMSO-d_6, 300 MHz) δ: 12.12(s, 1H), 8.00-8.20(m, 4H), 7.93-7.96(m, 2H), 7.77-7.80(m, 3H), 7.40-7.42(m, 5H), 7.23(t, *J*=15Hz, 2H), 6.15(s, 2H), 4.93-4.97(m, 2H) 3.95-4.01(m, 2H), 3.57(s, 3H); ^{13}CNMR(75 MHz, DMSO-d_6,) δ: 175.39, 151.22, 142.18, 137.84, 135.64, 134.92, 133.81, 132.24, 131.25, 130.98, 129.52, 128.71, 127.27, 126.89, 125.15, 123.69, 122.12, 119.88, 113.34, 113.06, 98.37, 70.34, 59.07, 50.95, 48.52, 40.75, 40.47, 39.91, 39.07; ESI-MS: *m/z* 488.2 $[M-Br]^+$,$C_{31}H_{26}N_3O_3^+$(MW=488.2); Anal.calcd for $C_{31}H_{26}BrN_3O_3\cdot 0.25HBr$ (587.20): C63.38, H4.97, N6.60; Found: C63.35, H4.69, N6.93.

*(E)-1-Benzyl-3-(2-methoxyethyl)-2-(4-hydroxy-3-methoxystyryl)-4,9-dioxo-4,9-dihydro-1H-naphth[2,3-d]imidazol-3-ium bromide (**12c**).*

Yield: 57.6%; brown powder; mp: 178-180°C; ^{1}H NMR(DMSO-d_6, 300 MHz) δ: 7.40-7.49(m, 9H), 7.32-7.34(m, 2H), 7.09(d, *J*=15Hz, 1H), 6.93(s, 1H), 6.51(d, *J*=15Hz, 1H), 3.87(s, 2H), 3.78-3.80(m, 2H), 3.75-3.76(m, 2H), 3.28(s, 3H), 3.25(s, 3H); ^{13}C-NMR (DMSO-d_6, 100 MHz) δ: ESI-MS: *m/z* 495.2 $[M-Br]^+$; Anal.calcd for $C_{30}H_{27}BrN_2O_5\cdot 1.3H_2O$ (597.40): C60.35, H4.72, N5.93; Found: C60.47, H5.01, N5.68.

*(E)-1-Benzyl-3-(2-methoxyethyl)-2-(3-hydroxystyryl)-4,9-dioxo-4,9-dihydro-1H-naphth[2,3-d]imidazol-3-ium bromide (**12d**).*

Yield: 72.9%; yellow powder; mp: 199-200°C; ^{1}H NMR(DMSO-d_6, 300 MHz) δ: 9.80(s, 1H), 8.00-8.20(m, 4H), 7.32-7.38(m, 5H), 7.27-7.30(m, 3H), 7.09(d, *J*=18Hz, 2H), 6.93(s, 1H), 3.87(s, 2H), 3.88(s, 2H), 3.57(s, 2H), 3.25(s, 3H); ESI-MS: *m/z* 465.2 $[M-Br]^+$,$C_{29}H_{25}N_2O_4^+$(MW=465.2); Anal.calcd for $C_{29}H_{25}BrN_2O_4\cdot 0.5H_2O$ (553.20): C62.81, H4.82, N4.46; Found: C62.82, H4.73, N4.68.

*(E)-1-(3-Methoxybenzyl)-3-(2-methoxyethyl)-2-(2-(1H-indol-3-yl)vinyl)-4,9-dioxo-4,9-dihydro-1H-naphth[2,3-d]imidazol-3-ium bromide (**12e**).*

Yield: 86.8%; purple red powder; mp: 196-197°C; ^{1}H NMR(DMSO-d_6, 300 MHz) δ: 8.20-8.22(m, 2H), 8.00-8.02(m, 2H),7.94(m, 1H), 7.68(d, *J*=9Hz, 1H), 7.53(d, *J*=9Hz, 1H), 7.35(t, *J*=9Hz, 1H), 7.18-7.29(m, 2H), 6.93-6.98(m, 3H), 6.12(s, 2H), 4.96(s, 1H), 3.94-3.97(m, 2H), 3.71(s, 3H), 3.57(s,3H); ^{13}C-NMR (DMSO-d_6, 100 MHz) δ: 174.92, 159.76, 141.72, 137.39, 135.99, 133.31, 131.71, 130.28, 126.79, 124.73, 123.21, 121.59, 119.41, 118.39, 113.31, 112.86, 112.63, 112.51, 97.88, 69.88, 66.33, 58.58, 55.12, 50.29, 47.99, 40.16, 39.95, 39.74, 39.53, 39.32, 39.11, 38.91; ESI-MS: *m/z* 518.2 $[M-Br]^+$,$C_{32}H_{28}N_3O_4^+$(MW=518.2); Anal.calcd for $C_{32}H_{28}BrN_3O_4\cdot 0.6H_2O$ (607.80): C63.32, H5.02, N6.52; Found: C63.08, H4.83, N6.90.

*(E)-1-(3-Methoxybenzyl)-3-(2-methoxyethyl)-2-(3,4,5-trimethoxystyryl)-4,9-dioxo-4,9-dihydro-1H-naphth[2,3-d]imidazol-3-ium bromide (**12f**).*

Yield: 50.9%; yellow powder; mp: 194-195°C; ^{1}H NMR(DMSO-d_6, 300 MHz) δ: 8.22-8.26(m, 2H), 8.00-8.03(m, 2H), 7.61(d, *J*=15Hz, 1H), 7.43(d, *J*=15Hz, 1H), 7.32-7.38(m, 1H), 7.03(s, 2H), 6.90-6.95(m, 3H), 6.15(s, 2H), 4.99(s, 2H), 3.86(s, 6H), 3.73(s, 3H), 3.31(s, 3H); ESI-MS: *m/z* 569.2 $[M-Br]^+$,$C_{33}H_{33}N_2O_7^+$(MW=569.2); Anal.calcd for $C_{33}H_{33}BrN_2O_7\cdot 2H_2O$ (684.20): C56.17, H5.56, N4.72; Found: C56.17, H5.30, N4.36.

*(E)-1-(3-Methoxybenzyl)-3-(2-methoxyethyl)-2-(3-hydroxystyryl)-4,9-dioxo-4,9-dihydro-1H-naphth[2,3-d]imidazol-3-ium bromide (**12g**).*

Yield: 61.5%; orange powder; mp: 204°C; ^{1}H NMR(DMSO-d_6, 300 MHz) δ: 9.80(s, 1H), 8.00-8.20(m, 4H), 7.53-7.57(m, 1H), 7.28-7.33(m, 3H), 7.09(d, *J*=15Hz, 2H), 6.90-6.94(m, 4H), 6.05(s, 2H), 4.94(s, 2H), 3.69(s, 3H), 3.25(s, 3H); ESI-MS: *m/z* 495.2

$[M\text{-}Br]^+$,$C_{30}H_{27}N_2O_5^+$(MW=495.2); Anal.calcd for $C_{30}H_{27}BrN_2O_5 \cdot 0.18HBr$ (588.60): C60.74, H4.68, N4.34; Found: C60.77, H4.62, N4.72.

4.3. Biological evaluation procedures

4.3.1. Drugs and drug treatments

Compound YM155 was used as is after purchasing from Zhongjiu Technology (Shanghai) Co. Ltd. Paclitaxel (Sigma, T7191) was dissolved in DMSO to make a stock concentration of 70 μM. Solutol® HS15, a nonionic solubilizer that consists of polyglycol mono- and di-esters of 12-hydroxystearic acid with approximately 30% of free polyethylene glycol, was purchased from BASF AG (Ludwigshafen, Germany) for making the injection solutions.

4.3.2. Cell lines and cultures

A375 (human malignant melanoma cell line), PC-3 (human prostate carcinoma cell line), Ramos (Human Burkitt's lymphoma cell line) and Hela (human cervical carcinoma cell line) were purchased from ATCC. The cells were cultured in DMEM, F12K and RPMI 1640 medium (Gibco), respectively, and supplemented with 10% fetal bovine serum (FBS) (Gibco), penicillin (100 U/mL), and streptomycin (100 μg/mL) in a humidified atmosphere of 5% CO_2 at 37°C.

4.3.3. Anti-proliferative assays

Cells were seeded into 96-well plates (100 μL of media containing 3000-10000 cells per well) and precultured for 1 day. Stock solutions (10 mM) of test compounds were prepared fresh by dissolving in DMSO. These solutions were used to prepare 10 μM of working solution, along with a 3-fold serial dilution in appropriate media. 100 μL of agent-containing media or control vehicle was added to each well. After 48 h of incubation at 37°C in a humidified atmosphere of 5% CO_2, cytotoxicity was determined using the CellTiter 96 Aqueous One Solution Reagent (Promega, USA) according to the manufacturer's instructions. The detection is based on the cellular conversion of a tetrazolium salt into a soluble formazan product as a measure of proliferation. The absorbance was measured at 492 nM by the Tecan Sunrise Microplate Reader (Tecan, Switzerland). Cellular response curves and IC_{50} values were calculated from the data.

4.3.4. Apoptosis detection assays

A375 cells were grown in the absence or presence of different concentrations (10, 100 and 1,000 nM) of **12b** for 24 h. For FACS analysis, cells were treated with either **12b** or YM155 for 24 h and then stained with Annexin V and propidium iodide using the Annexin V/propidium iodide apoptosis kit per the manufacturer's instructions (Biouniquer, BU-AP0103). Data were acquired using a FACSCalibur system (BD Biosciences) and analyzed by FlowJo software.

4.3.5. Western blot analysis

A375 cells (1×10^5 cells/well) were seeded into 6-well culture plates. After treatment with **12**b or YM155 at the indicated concentration for 48 h, the media was removed and cells were immediately lysed in RIPA Lysis Buffer (Beyotime, P0013B). The resulting lysates containing equal amounts of protein were boiled in sodium dodecyl sulfate (SDS)-sample buffer for 5 min before loading on a 12% SDS-polyacrylamide gel. Proteins were electro-transferred to a polyvinylidene difluoride (PVDF) membrane and blocked in PBS containing 5% non-fat dry milk for 1 h at room temperature. Primary antibodies used included a polyclonal antibody to Survivin (Novus biologicals, NB500-201), caspase-3 (Cell Signaling Technology, 9662S), Bcl-2 (Cell Signaling Technology, 2876), PARP (Beyotime, AP102), p-ERK (Cell Signaling Technology, 4695), and total-ERK (Cell Signaling Technology, 9101) as well as a monoclonal antibody to GAPDH (Beyotime, AG019) at a 1:1000 dilution. Secondary antibodies used included anti-rabbit IgG peroxidase conjugate (Sigma, A0545) and anti-mouse IgG peroxidase conjugate (Sigma, A2554). Bands were visualized using the ECL system (PerkinElemer, NEL104001EA), and pictures were taken using the Bio-Rad ChemiDoc XRS System.

4.3.6. Caspase activity assay

Cells were seeded at 8×10^3 cells/well and treated with the test compounds at 1000 nM. Subsequently, caspase 3/7 activity was measured to gauge cell apoptosis as determined by the Caspase-Glo 3/7 assay kit (Promega) following the manufacturer's instructions. Luminescence was detected using a Tecan Infinite 200 microplate reader (Tecan, Switzerland).

4.3.7. Cell cycle arrest assay

Cell cycle arrest was analyzed by flow cytometry. Briefly, A375 cells (2×10^5 cells/well) were seeded into 6-well plates and exposed to various concentrations of compounds **12b** (0, 100, 200 and 400 nM). At appropriate intervals, treated and control cells were harvested by trypsinization and centrifuged at 4°C. Cell pellets were washed twice with phosphate buffered saline (PBS) and fixed in 70% ice-cold ethanol at -20°C until all time points had been collected for analysis. The samples were concentrated by removing EtOH and staining the cellular DNA with PI/RNase Staining Buffer (BD, 550825) for 30 min at 4°C in the dark. The cell cycle distribution was detected using a FACScan Flow Cytometry (BD FACSCalibur) with 10,000 events per determination, and the DNA content of the cells was analyzed using the Modfit LT program (Verity Software, USA).

4.3.8. Immunofluorescence staining

All reagents for fixation, wash, and blocking steps were purchased from Beyotime (Beyotime). A375 cells (8×10^3 cells/well) were maintained in black 96-well microplates (Corning, 3603) and treated with DMSO, **12**b, YM155 or Paclitaxel for 24 h at 37°C. Samples were fixed, blocked, and permeabilized after being washed. Cells were subsequently incubated with monoclonal α-tubulin

primary antibody (Beyotime, AT819) overnight, washed extensively, and incubated in FITC-labeled secondary antibody (Invitrogen, 626511) for 3 h. Nuclei were labeled with DAPI. Images of fluorescently labeled tubulin and nuclei were captured on an ImageXpress 5000A automated cellular imaging and analysis system (Molecular Devices).

4.3.9. Antitumor evaluation in mice

Adult male ICR mice, 6 weeks old and weighing 20-25 g, were purchased from the Experimental Animal Center of Yangzhou University. The mice were housed in polycarbonate cages under standard laboratory conditions (24±1°C, 12 light/dark cycle) with food and water *ad libitum*. All procedures used for animal experimentation were approved by the China Pharmaceutical University Institute Animal Care and Use Committee. Preliminary experiments determined the maximum tolerated dose of compound **12b** to be 1.0 mg/kg in non-tumor-bearing animals. YM155 and **12b** were freshly prepared daily using the formulation solvent containing saline, 4% N, N-Dimethylacetamide (DMA), and 2% Solutol® HS15. Cyclophosphamide (CTX) was diluted with only saline. All the solutions were injected intraperitoneally in a volume of 0.1 mL per 10 g of body weight.

Ehrlich ascites carcinoma (EAC) is an undifferentiated carcinoma, originally hyperdiploid, and has high transplantable capability, rapid proliferation, shorter life span and 100% malignancy. EAC resembles human tumors that are most sensitive to chemotherapy because they are undifferentiated and have a rapid growth rate [28]. A fixed number of viable EAC cells (1×10^6 cells/22 g b. wt) were implanted into the peritoneal cavity of each donor mouse. The tumor cells were then withdrawn, diluted in sterile saline, counted and inoculated (5×10^6 cells/animal) to the right thigh of experimental animals by subcutaneous (s.c.) injection for the development of solid tumor [29].

The day of tumor implantation was considered day 0. On day 1, animals were randomly divided into five groups (n=7 each) and administered with or without compound **12b** by intraperitoneal (i.p.) injection for 10 d: (1) Vehicle control group: only formulation; (2) CTX group: 30 mg/kg/day of CTX; (3) 12b-1 group: 0.06 mg/kg/day of **12b**; (4) 12b-2 group: 0.2 mg/kg/day of **12b**; and (5) 12b-3 group: 0.6 mg/kg/day of **12b**. Mice with subcutaneous solid tumors were weighed every day. At the end of the experiment, mice were sacrificed and their tumor masses and important organs dissected and weighed.

4.3.10. Experimental design and data analysis

Dose-response curves were analyzed using the GraphPad Prism™ 5 software program to calculate IC_{50} values using a three-parameter logistic equation. Data were expressed as the mean and standard deviation. The statistical significance of the differences observed in the results of the independent experiments was analyzed using the Student's *t*-test. A *p*-value of <0.05 was considered statistically significant.

References

[1] D.C. Altieri, Cancer letters, 332 (2013) 225-228.

[2] W.G. Herrington, D.C. Talbot, M.M. Lahn, J.T. Brandt, S. Callies, R. Nagle, C.G. Winearls, I.S. Roberts, American journal of kidney diseases : the official journal of the National Kidney Foundation, 57 (2011) 300-303.

[3] E. Park, E.J. Gang, Y.T. Hsieh, P. Schaefer, S. Chae, L. Klemm, S. Huantes, M. Loh, E.M. Conway, E.S. Kang, H. Hoe Koo, W.K. Hofmann, N. Heisterkamp, L. Pelus, G. Keerthivasan, J. Crispino, M. Kahn, M. Muschen, Y.M. Kim, Blood, 118 (2011) 2191-2199.

[4] S. Gross, V. Lennerz, E. Gallerani, N. Mach, S. Bohm, D. Hess, L. von Boehmer, A. Knuth, A. Ochsenbein, U. Gnad-Vogt, U. Forssmann, T. Woelfel, E. Kaempgen, Cancer immunology research, 4 (2016) 18-25.

[5] M. Karkada, N.L. Berinstein, M. Mansour, Biologics : targets & therapy, 8 (2014) 27-38.

[6] T. Nakahara, M. Takeuchi, I. Kinoyama, T. Minematsu, K. Shirasuna, A. Matsuhisa, A. Kita, F. Tominaga, K. Yamanaka, M. Kudoh, M. Sasamata, Cancer research, 67 (2007) 8014-8021.

[7] X. Ling, S. Cao, Q. Cheng, J.T. Keefe, Y.M. Rustum, F. Li, PloS one, 7 (2012) e45571.

[8] A.M. Smith, E.B. Little, A. Zivanovic, P. Hong, A.K. Liu, R. Burow, C. Stinson, A.R. Hallahan, A.S. Moore, Leukemia research, 39 (2015) 435-444.

[9] A. Rauch, D. Hennig, C. Schafer, M. Wirth, C. Marx, T. Heinzel, G. Schneider, O.H. Kramer, Biochimica et biophysica acta, 1845 (2014) 202-220.

[10] N. Nakamura, T. Yamauchi, M. Hiramoto, M. Yuri, M. Naito, M. Takeuchi, K. Yamanaka, A. Kita, T. Nakahara, I. Kinoyama, A. Matsuhisa, N. Kaneko, H. Koutoku, M. Sasamata, H. Yokota, S. Kawabata, K. Furuichi, Molecular & cellular proteomics : MCP, 11 (2012) M111 013243.

[11] T. Yamauchi, N. Nakamura, M. Hiramoto, M. Yuri, H. Yokota, M. Naitou, M. Takeuchi, K. Yamanaka, A. Kita, T. Nakahara, I. Kinoyama, A. Matsuhisa, N. Kaneko, H. Koutoku, M. Sasamata, M. Kobori, M. Katou, S. Tawara, S. Kawabata, K. Furuichi, Biochemical and biophysical research communications, 425 (2012) 711-716.

[12] Q. Cheng, X. Ling, A. Haller, T. Nakahara, K. Yamanaka, A. Kita, H. Koutoku, M. Takeuchi, M.G. Brattain, F. Li, International journal of biochemistry and molecular biology, 3 (2012) 179-197.

[13] D.N. Church, D.C. Talbot, Current oncology reports, 14 (2012) 120-128.

[14] R.J. Kelly, A. Thomas, A. Rajan, G. Chun, A. Lopez-Chavez, E. Szabo, S. Spencer, C.A. Carter, U. Guha, S. Khozin, S. Poondru, C. Van Sant, A. Keating, S.M. Steinberg, W. Figg, G. Giaccone, Annals of oncology : official journal of the European Society for Medical Oncology / ESMO, 24 (2013) 2601-2606.

[15] N. Singh, S. Krishnakumar, R.K. Kanwar, C.H. Cheung, J.R. Kanwar, Drug discovery today, 20 (2015) 578-587.

[16] R. Mikstacka, T. Stefanski, J. Rozanski, Cellular & molecular biology letters, 18 (2013) 368-397.

[17] J. Jiang, C. Zheng, K. Zhu, J. Liu, N. Sun, C. Wang, H. Jiang, J. Zhu, C. Luo, Y. Zhou, Journal of medicinal chemistry, 58 (2015) 2538-2546.

[18] Y. Shan, J. Zhang, Z. Liu, M. Wang, Y. Dong, Current medicinal chemistry, 18 (2011) 523-538.

[19] G.C. Tron, T. Pirali, G. Sorba, F. Pagliai, S. Busacca, A.A. Genazzani, Journal of medicinal chemistry, 49 (2006) 3033-3044.

[20] H. Rajak, P.K. Dewangan, V. Patel, D.K. Jain, A. Singh, R. Veerasamy, P.C. Sharma, A. Dixit, Current pharmaceutical design, 19 (2013) 1923-1955.

[21] D. Renko, O. Provot, E. Rasolofonjatovo, J. Bignon, J. Rodrigo, J. Dubois, J.D. Brion, A. Hamze, M. Alami, Eur J Med Chem, 90 (2015) 834-844.

[22] P. Signorelli, R. Ghidoni, The Journal of nutritional biochemistry, 16 (2005) 449-466.

[23] M.A. Reddy, N. Jain, D. Yada, C. Kishore, J.R. Vangala, P.S. R, A. Addlagatta, S.V. Kalivendi, B. Sreedhar, Journal of medicinal chemistry, 54 (2011) 6751-6760.

[24] P. Truitt, D. Hayes, L.T. Creagh, Journal of medicinal chemistry, 7 (1964) 362-364.

[25] A.R.D. J. R. E. Hoover, J. Am. Chem. Soc., 76 (1954) 4148-4152.

[26] S.C. Kuo, T. Ibuka, L.J. Huang, J.C. Lien, S.R. Yean, S.C. Huang, D. Lednicer, S. Morris-Natschke, K.H. Lee, Journal of medicinal chemistry, 39 (1996) 1447-1451.

[27] S.R. Punganuru, H.R. Madala, S.N. Venugopal, R. Samala, C. Mikelis, K.S. Srivenugopal, Eur J Med Chem, 107 (2016) 233-244.

[28] M. Ozaslan, I.D. Karagoz, I.H. Kilic, M.E. Guldur, African Journal of Biotechnology, 10 (2011) 2375-2378.

[29] R.R. Somasagara, M. Hegde, K.K. Chiruvella, A. Musini, B. Choudhary, S.C. Raghavan, PloS one, 7 (2012) e47021.

[30] A. Matsuhisa, I. Kinoyama, A. Toyoshima, T. Nakahara, M. Takeuchi, M. Okada, Fused imidazolium derivatives, in, 2003.

Synthesis and biological evaluation of novel 2-arylvinyl-substituted naphtho[2,3-*d*]imidazolium halide derivatives as potent antitumor agents

Qingyun Wei[a], Ju Li[a], Feng Tang[b], Yin Yin[b], Yong Zhao[b, **], Qizheng Yao[a, *]

[a] Department of Medicinal Chemistry, China Pharmaceutical University, Nanjing 210009, PR China

[b] MtC Biopharma, Co., Ltd, Nanjing 210042, PR China

Highlights

- **Two series of 2-arylvinyl-substituted naphtho[2,3-d]imidazolium derivatives were designed and synthesized.**
- **Compound 12b exhibited potent antiproliferative activity.**
- **Compound 12b induced cell apoptosis and affected microtubule networking.**
- ***In vivo* 12b inhibited subcutaneous solid tumor growth.**